Development of a Smart Underwater "Wet" Welding Process

Chon L. Tsai, Chong H. Jiang, Daein Kang, and Bao T. Song, *1996*
The Ohio State University

Technical Bulletin Series
OHSU-TB-033

Ohio Sea Grant College Program
1997

Made available by:
Ohio Sea Grant College Program
The Ohio State University
1314 Kinnear Road
Columbus, OH 43212-1194
614/292-8949, Fax 614/292-4364
http://www-ohiosg.osc/OhioSeagrant

Funding support

This publication (OHSU-TB-033) is a result of the research project "**Development of a smart underwater 'wet' welding process**" that was partially supported by Ohio Sea Grant College Program (project R/OE-11, grant NA46RG0482) from the National Sea Grant College Program of the National Oceanic and Atmospheric Administration (NOAA), U.S. Department of Commerce.

Ohio Sea Grant also receives support from is also provided by the Ohio Board of Regents, The Ohio State University, Ohio State University Extension, and participating universities. The Ohio Sea Grant College Program is administered by The Ohio State University.

Report

October 31, 1996

OSU RF Project Number 729734-Final Report
Project Duration: September 1, 1994 to August 31, 1996

Final Report

ON

DEVELOPMENT OF A SMART UNDERWATER "WET" WELDING PROCESS

Submitted to

Ohio Sea Grant College Program
The Ohio State University
1314 Kinnear Road
Columbus, Ohio 43212-1194

by

Chon L. Tsai, Chong H. Jiang and Daein Kang
Department of Industrial, Welding and Systems Engineering
The Ohio State University

Bao T. Song
Harbin Research Institute of Welding, P.R.C.

EXECUTIVE SUMMARY

For underwater wet welding, the improvement of manual methods and systems are necessary since fully mechanized and automatic repair are not always available for already existing pipelines and offshore structures. A suitable method must be available for emergency repair work. The development of fully mechanized methods will take a long time before they are operationally ready. Recent investigation indicates that wet semi-automatic flux cored arc welding process will show the greatest potential.

In this project, automatic flux cored arc welding was first conducted underwater to eliminate human factors. The base metal used was a ASTM A36 mild steel, the filler materials were two ferritic steel wires and an austenitic stainless steel wire. Before the underwater wet welding, the welding gun was waterproofed with the addition of O-ring gaskets placed at the bottom of the head tube and within the nozzle extension. A gas cup unit was developed to get a better shielding effect of the wet welds. Two sets of gas cup with the same design were made, one set is made or brass, for general purpose applications, another set made of plastic, for the embedding of thermal couples to monitor the average temperature inside the dynamic bubbles. Originally, both carbon dioxide and compressed air were tested for the shielding purpose, after a series of evaluations, compressed air was chosen as the shielding gas. A blanket made of aluminum was also designed aiming at slowing down the cooling rate of the weld zone at a critical temperature range by the water environment. After welding, comprehensive evaluations were carried out on the wet welds, including chemical analysis, metallurgical evaluation, hardness survey, mechanical property tests and fracture analysis.

During the tests, it was observed that, for underwater wet welding, a higher heat input, more precisely a higher arc voltage level is needed to achieve a weld with acceptable bead appearance, weld contour and weld properties. This is thought to be caused by two factors: the fast cooling rate and the lower wettability of the liquid metal on the surface of the base metal in a water environment. Both chemical and metallurgical evaluations of the welds showed that the change in weld metal microstructure of the stainless steel wire may be caused by the change of solidification modes instead of the change of weld metal chemical composition. No weld metal and heat-affected zone cracks were observed for both the ferritic steel wires and austenitic stainless steel wire made

underwater. Mechanical property test results show that maximum strain to failure of the all weld metal tensile test samples especially the one of the stainless steel welds was almost the same as the air weld, the bending ductility of the wet welds were much better than that of other underwater wet welds.

The concept of a smart wet underwater welding process was proved very successful. It seems that the finalized smart process will integrate the flexibility of the manual welding process, the feedback control of the automatic welding process and the slow cooling rate of the semi-dry welding process. It is the addition of the gas cup unit and the shielding gas that makes the improvement of the performance of the electrodes tested underwater. With the addition of the gas cup unit and the shielding gas, the partially mixed zone in the weld metal of the austenitic stainless steel wire is the narrowest in comparison to those of the air welds and underwater wet welds without the addition of the gas cup unit. Penetration is greatest when no gas cup unit and shielding gas were used. The introduction of the average temperature monitoring of the dynamic bubbles makes it possible for the implementation of the feedback control of the smart underwater wet welding process. More benefits will be obtained from the new smart underwater wet welding process in the future, with further development of the process.

Table of Contents

Page

ACKNOWLEDGMENTS

This project was completed under the financial support of the Ohio Sea Grant College Program. The researchers would like to acknowledge the numerous invaluable contributions, comments and advise of Dr. Jeffrey Reutter, Maran Hilgendorf of the Ohio Sea Grant College Program, and Mr. William Svekric of Welding Consultants, Inc.

The researchers acknowledge Mary Hartzler, Bob Miller and Nils Theller of The Ohio State University, for their dedicate machining work. Additional acknowledgment is extended to Larry Stahr of Edison Welding Institute, for his assistance in metallographic work, Luke Yoder, Jeff Glazer and Tim Wampler for their valuable suggestions and help during the experimental work.

The researchers would also like to thank Brian Hart, Mike Sartin and mark Busby of Welding Consultants, Inc. for their many contributions to the project. It would have been impossible to conduct the experimental tests without them.

1.0 INTRODUCTION

1.1 Background

Current underwater welding technology can produce "code-quality" welds if a dry chamber system is used. But the large pressurized air chamber used to exclude water from the work area has high operational costs which make the process economically unfeasible. The alternative to the "dry" welding process is the "wet" welding process performed manually. However, the economic advantage of this simple welding process must be offset by the adverse effects of the water environment. The water environment greatly restricts the visibility of the welder and the freedom of manipulation of the welding process. In addition, underwater "wet" welds are plagued by the rapid quenching effect of the surrounding water and by a susceptibility to hydrogen embrittlement. In comparison to their in-air counterparts, the inferior quality of underwater "wet" welds due to rapid quenching and hydrogen embrittlement is well known. These two inherent problems remain today[1-4].

Since 1985, the proposer has taken a new approach to the underwater "wet" welding problems. A series of research programs, individually sponsored or co-sponsored by the Ohio Sea Grant College Program, The Thomas Edison Program of the State of Ohio, National Coastal Research Institute, The Ohio State University and two Ohio companies, have resulted in the development of a fitness-for-service design solution, including a new design methodology and an improved underwater "wet" welding electrode[5-8]. This design approach can fulfill underwater structural requirements using the existing underwater "wet" welding technology.

As part of a parallel effort to the design solution, the operational efficiency and the "wet" weld quality can be improved through process development. A smart underwater "wet" welding process, which will ease the visibility and manipulation difficulties when welding in an open-water environment, can be developed using a semi-automatic process, pressure and temperature sensors, and the same "wet" welding principles. This system could then be packaged and used as a unit.

1.2 OBJECTIVES

The objectives of this project are threefold: 1) Develop the smart underwater welding system based on existing technology, 2) Establish technical data to support the use of this smart system, and 3) Demonstrate and disseminate the technology to the industrial users.

1.3 METHODOLOGY

The smart underwater welding process requires modifying existing flux-cored arc welding technology with the following design characteristics:

1) The flux ingredients must produce sufficient gas of low ionization potential to maintain a stable welding arc. The flux ingredients must also counteract the water environment effects by containing appropriate chemicals to reduce the hydrogen effect and alloying elements to enhance the physical and metallurgical properties of the weldment. The weld quality resulting from this study will be measured by the requirements of the American Welding Society D3.6-93 Specifications (AWS D3.6)[9], Type "A" welds.

2) The Welding gun must have the ability to sense the bubble stability and, through a feedback linkage, control the welding current and electrode feed rate to ensure sufficient energy to produce the appropriate amounts of gas generation.

3) The welding gun must be self-contained with the filler wire and wire feed system as an integrated part of the gun. The gun must be designed for easy manipulation and with an illuminated transparent gas cup for the diver/welder to visually track the joint. A seam tracking device may be an alternative but this may complicate the welding gun and reduce the manipulability.

4) A gas blanket to be dragged behind the gun can reduce the weld metal cooling rate and enhance the weld properties. It has been reported that energy loss from the weld behind the arc is responsible for rapid cooling of the underwater wet welds (Tsai et al. 1979). Therefore, a means to create a stable gas film covering the weld behind the arc would reduce the cooling rate.

Using the flexible gas blanket is conceptually feasible but needs to be investigated.

The smart underwater welding process uses the flux-cored arc welding principles which produces coalescence of metals by heating them with an arc between a continuous tubular metal (consumable) electrode and the work. Shielding is provided by a flux contained within the tubular electrode. The vaporized flux ingredients produce shielding gas which displaces water by forming dynamic bubbles, thus protecting the arc and the molten weld pool during welding. The deoxidizing constituents in the flux counteract the humidity and pressure effects and improve the weld properties.

Researchers at E.O. Paton Electric Welding Institute in Kiev, Ukraine have studied underwater "wet" welds made by the flux-cored arc welding process since 1974. This welding process has been used for repair of cracked pipelines at a depth of 10 to 12 meters. The impact strength of weld metal was reported having an average Charpy-V notch value of 43 ft-lbs at 0 degree celsius and 28 ft-lbs at -20 degree Celsius. These test results would qualify the flux-cored "wet" welds for the AWS D3.6 Specifications, Type "A" welds. Unfortunately, the impact values of the heat-affected zone were not reported. It must also be noticed that the favorable assessment of weld metal impact strength of the flux-cored "wet" welds was based on limited number of Charpy tests.

The flux-cored arc welding wires manufactured by E.O. Paton and Hobart Brothers, a U.S. company, have been tested at the Ohio State University Welding Engineering Laboratory. Neither filler wires performed well. The Paton process has also been tested and evaluated by several US companies where the reported results by the Paton Institute could not be reproduced. In addition, information on chemistry designs of the Paton welding flux has been kept as a commercial secret. The fundamental understanding of the relationships among the flux chemistry, the welding process parameters, and the resulting weld quality is not available. Therefore, in addition to the development of a practical underwater welding process, the proposed project will also develop the engineering knowledge of the flux-cored arc welding technology used underwater.

Several factors will be studied during the developmental course of the smart system. They are the parameter control

database (e.g. water depth effect), gun design, dynamic bubble characteristics, flux chemistry, and working range of the welding parameters. To ensure practical use of the project results by the industrial users, the parameter control database which shows the common operational ranges of the underwater welding work will be developed. This parameter control database defines the underwater operation conditions under which the new underwater welding process can be qualified for industrial applications. This database will set the limits for the factorial studies in the development of the smart underwater welding process.

2.0 LITERATURE REVIEW

2.1 General

Underwater welding can be classified into three categories: dry underwater welding, locally dry underwater welding and underwater wet welding. Dry underwater welding requires that the water surrounding the work be eliminated, normally by use of a pressurized enclosure with controlled atmosphere and pressure. The dry process is costly, but produces welds which are generally equal in quality to welds made above water. The locally dry techniques, by means of which the welding site is shielded by an independently supplied gas atmosphere, have been developed especially for the application of inert gas welding methods[10]. The gas cavity is thereby supported by appropriate measures. The new underwater welding techniques that mainly used in marine engineering in recent years were the wet welding with stick electrode and the locally drying CO_2 semiautomatic arc welding process[11]. Underwater wet welding is done at ambient pressure with the welder-diver in the water without any mechanical barrier between the water and the welding arc. The shielded arc process is commonly used.

The versatility, speed, and lower cost of wet welding makes the process highly desirable for underwater welding when "average" quality is acceptable. Wet welding can be accomplished without special fixturing. Where repair needs are the greatest-in salt water areas-the success of wet welding is greatly enhanced, since the higher the salinity of the water the greater the stability of the wet welding process. The dissolved salts in the water increase its electrolytic qualities, thus enabling a hotter arc and a more efficient welding operation. Still the use of underwater wet welding is restricted by the low quality of the welds, which do not fulfill the higher quality specifications of the AWS standard. Therefore, further investigations and improvements of wet underwater welding are necessary.

2.2 Weldability Considerations in Underwater Wet Welding

2.2.1 Thermal Experience

Brown and Masubuchi[1] developed a model for the heat transfer process involving the energy input from the welding source and the energy input from the welding source and the energy losses to the environment during underwater welding. These investigators hold that boiling and radiation account for the major heat losses from the plate. The bubbles generated during welding carry considerable heat as they leave the plate and are responsible for the faster cooling rates experienced in underwater wet welding. Thus, the cooling rate, expressed as the time it takes to cool from 800 to 500 °C , is approximately two to four times faster than in surface welding[12]. Hamann and Mahrenholts[13] investigate the influence of the surface heat transfer on the temperature distribution during wet underwater welding, and the results show that the neglecting of undercooled boiling leads to cooling velocities that are too small.

The arc efficiency, and by consequence the effective heat input, is affected by depth. Avilov[14] determined that the constriction of the arc caused by the water head results in a decrease in current which in turn raises the voltage of the welding machine in order to maintain a constant power. Ibarra[15] investigated the effect of depth on the arc characteristic and reported that as depth increases the arc characteristic curve intersects the drooping characteristic curve, of a constant current source, at decreasing currents. This decrease in current reduces the heat input since in practice the power is not actually maintained constant, and consequently faster cooling rates may be obtained.

2.2.2 Hydrogen Cracking

The necessary conditions for hydrogen-induced cracking require sufficient hydrogen, susceptible microstructures, high stresses and sensitive temperature range in the weld. These conditions all exist in the wet welds. For wet welding it has already been stated that the weld hydrogen level is dramatically increased and therefore the risk of cracking in underwater weldments made in the wet is also dramatically increased[16-18].

Although there is little information to provide guidance as to the likely changes in the level of residual stress in underwater welds compared to those made in the air, it is expected that in wet welding the local quenching effects may alter both the distribution and magnitude of residual stresses although the extent of any such changes has not been determined.

In general the harder the microstructure the greater the susceptibility to hydrogen cracking. Any increase in cooling rate through the transformation temperature range will increase HAZ and weld hardness and hence increase the risk of cracking. In wet welds the dramatic increase in cooling rate and therefore hardness would result in an increased risk of cracking. Any changes in the arc efficiency, i.e. rates of arc energy consumed converted to heat into the plate, would also be expected to affect the cooling rate for better or worse depending on the change in efficiency.

2.2.3 Solidification Cracking

The principal controlling compositional factors in solidification cracking are now established[19]. Thus, increase in weld metal, C, S, and P levels and decreases in Mn level increase the risk of solidification cracking. As a results of pressure increases the kinetics and equilibrium of normal weld pool chemistry reactions will be expected to change. In wet welding, one results of the higher oxygen levels may be a resultant decrease in carbon content and in the level of deoxidants such as manganese and silicon, lower manganese levels certainly being detrimental with respect to solidification cracking.

2.2.4 Toughness

Weld Metal

Good toughness results from the balance of a fine-grained microstructure and a low yield strength giving high resistance to cleavage and from a low inclusion content giving good resistance to ductile fracture. Any compositional changes which result in harder microstructures, i.e. of higher yield strength, without an improvement in microstructural features, e.g. refinement of

acicular ferrite grain size, reduction in amount of proeutectoid ferrite, or upper bainite, would be detrimental, particularly to the cleavage resistance. Any compositional changes which would result in a higher inclusion content would be expected to be detrimental to the resistance to ductile tearing which may be of particular importance in respect of passing bend test requirements. For wet welds where dramatic increases occur in weld cooling rate and presumably weld solidification rates, the trapping of inclusions within the weld metal which in air weld would have floated out to the slag may also increase inclusion content and reduce the resistance to ductile tearing, as well as raising the hardness and yield strength and hence resistance to cleavage.

Heat Affected Zone

No compositional changes in the HAZ would be expected apart from a relatively transient increase in hydrogen level. In normal fabrication welds the hydrogen introduced into the HAZ from the weld diffuses away to sufficiently low levels so that by the time the weld experiences service stresses no detrimental effects of any remaining hydrogen are normally observed. Even repair welds made under normal ambient welding conditions, which may be stressed more rapidly after welding than normal fabrication welds, have not indicated any problems. However, in repairs to many offshore installations the repair welds may see service stresses very soon after being made and the effect of the transient increase in hydrogen level on fracture toughness would need to be evaluated. In wet welding where cooling rates are very much enhanced resulting in considerably harder HAZs, in general a detrimental influence on the HAZ toughness would be expected, although detailed changes would depend on actual compositions.

2.2.5 Fatigue

The fatigue strength of welded joints is almost entirely controlled by the stress concentrating effects of weld shape, undercut, and sharp slag intrusions, etc. in the fusion boundary region[20], particularly if the weld is left unground or unmachined. The extent to which either weld bead shape deteriorates, i.e. decrease in contact angle and hence increases in local stress concentration occur, or slag intrusions at the toes of the weld are made deeper, for underwater welding of any

type, should be considered since both of these factors could decrease the fatigue life of a welded joints. Some research work had been done at the Ohio State University regarding the wet welds geometry and the fatigue strength of the cruciform joints[21].

2.2.6 Porosity

The increase in the quality and size of weld pores with increasing depth has been documented by every investigator of wet welding. Ibarra, et al.[15], proposed a theoretical approach to the determination of the critical pore size as a function of pressure. The formation of these pores is controlled by the solubility of the various gases (principally hydrogen) in the molten metal. Subsequent rapid cooling reduces the solubility and rejects the dissolved gases as molecules which form bubbles in the molten metal. Wet welding solidification is so rapid as to prevent these bubbles from rising to the surface of the molten metal and escaping, thus being trapped within the solidified metal. These pores reduce the net section of the weld causing a reduction in strength, ductility and toughness.

2.3 Underwater Wet Welding Processes

There are several wet welding processes presently employed or under development. They are shielded metal arc welding (SMAW), gas metal arc welding (GMAW), flux-cored arc welding (FCAW), explosive welding (EW), friction welding (FW), and stud welding (SW). Recently, other welding processes such as laser welding[22], friction stud welding[23], "MOSS" modular orbital welding system[24]. Underwater robotic arm by graphical simulation techniques were also used[25]. The SMAW process is the most widely used of all the underwater welding methods.

The improvement of manual methods and systems is necessary since fully mechanized and automated repair methods which are not always available for already existing pipelines and offshore structures. A suitable method must be available and usable particularly for emergency repair work. The development of fully mechanized methods will take years if not decades before such methods are operationally ready. Even if fully mechanized or automated systems exist in the future, the use of human resources under water will continue to be necessary for special tasks. It

is expected that the semi-automatic flux-cored arc welding process will show the greatest potential.

Researchers in the former USSR were actively performing research with the flux cored process. The first reported usage of the process underwater was by Avilov[26] who described attempts in improving the quality of SMAW underwater welds by using flux coated tubular electrodes with argon gas forced through the core. Even though this early attempt did not improve the quality of underwater welds this work did provide new ideas and methods for others to build from.

The first quality underwater FCAW welds were reported by Savich[27] in 1969. His research was also based on the study of how alloying elements transfer across the welding arc, but in this case a flux cored electrode was used for the research. Savich then compared these results to a similar study in air to determine the difference in the transfer of alloying elements and determined that only the transfer of carbon, manganese, and silicon were significantly different. because arc current, voltage, and travel speed had been shown to affect the transfer of these three elements in SAW welding in air, Savich also performed similar studies for underwater welding.

From previous studies of the effects of water vapor decomposition, rapid cooling rates, and arc stability in underwater welding, a special flux was developed. Although the exact composition of this flux is not known, it is clearly the key to the success of these electrodes. Regardless of how the exact formulation of this electrode it remains as one of the single most effective underwater FCAW electrode that has been developed to date.

2.4 Underwater Wet Welding Consumables

Although no commercial welding electrode has been found to satisfy AWS D3.6 Type-A requirements, there are several electrodes that could satisfy Type-B standards[9]. Many efforts have been made on the improving and evaluation of the underwater wet welding consumables[28-34]. The commercial and experimental SMAW electrodes for underwater wet welding can be classified into three main categories (according to the type of filler metal used): ferritic, austenitic, and nickel based. Ferritic

electrodes are generally used for welding steels of carbon equivalent less than 0.4 down to depths of 100 m. Since austenitic stainless steel and nickel based filler metals have higher hydrogen solubility, making them less susceptible to hydrogen-induced cracking, they are used in the welding of higher carbon equivalent steels. However, even with the nickel based electrode, hydrogen-induced cracking in HAZs can not be completely avoided if the carbon equivalent of the base metal is higher than 0.4[33].

2.5 Approaches to Weld Metal Integrity

2.5.1 Microstructural Refinement

The electrode selection for underwater wet welding currently consists of matching existing commercial electrodes to the particular structural requirements of the repair. Through microstructural refinement of the weld metal, it is possible to increase toughness and compensate for porosity. This is possible to through the promotion of acicular ferrite with the addition of some microalloying elements, such as titanium and boron to the flux coating of the electrodes.

2.5.2 Porosity Minimization

According to the literature[30,32], the main components of the gas in a pore are hydrogen, carbon dioxide, carbon monoxide, hydrogen gas, etc. In theory, if the activity of these gases is reduced, the amount of hydrogen in the weld metal can also be reduced. Chew[35] and Gretskii[36] have shown that it is possible to decrease the amount of weld metal diffusible hydrogen by increasing the amount of calcium carbonate in the electrode covering. As calcium carbonate decomposes, gases other than hydrogen, in particular CO, reduce the partial pressure of hydrogen.

Ibarra, et al[15], argued that, since the weld metal carbon pick up increases with depth, the use of electrodes with calcium carbonate additions to reduce porosity should be restricted to shallow waters. An alternative method would be the addition of zeolites (which can be charged with inert gases) to the flux. These materials may, upon decomposition, release the argon or helium charged prior to welding, which can reduce the relative concentration of hydrogen.

2.5.3 Design Approach

The design criteria approach is based on the assumption that all underwater welds have inferior properties than their in-air counterparts. A flexible intermediate connection pad (prefabricated on land), which was developed at the Ohio State University[8], is wet welded to the structural member to cushion the stresses on the weld joints. Minimizing the stresses and reducing the cracking susceptibility of the welded structures.

The design approach , together with understanding of the mechanical properties of "wet" welds, has been demonstrated to be effective in achieving the intended structural performances of the welded joints using the improved electrodes[8]. The design approach to the structural problems associated with the "wet" welds was demonstrated by three ship repair examples, and it is concluded that underwater wet welds can be used in their present state for structural repair or construction if a proper design procedure, such as the procedures currently used by the US Navy, are used then underwater wet welding can be used without any modifications. Through proper design the wet welded joints will fit for their intended service without compromising the economical advantages[33].

2.5.4 Other Measures

Suga[37] studied the effect of cooling rate on mechanical properties of underwater wet welds in gravity arc welding, and indicated that the weld joints obtained by oil putty shielding have nearly comparable mechanical properties with those of open air welds. Hutt et al.[38] reported that hot tapping was used on a subsea pipeline, where a unique induction heating system to provide continuous preheating of the weld zone under extreme line flow and pressure conditions was applied. The system, together with a number of other special techniques, was employed in October 1994 for the subsea installation of a 36in. by 16in. tee on the Den Helder gas trunkline.

3.0 EXPERIMENTAL PROCEDURE

3.1 Approach and Procedures

All the studies at this stage are based on the weld plates made underwater in the water tank using the automatic flux-cored arc welding process(FCAW). For comparison, air welds also were made. After welding, chemical, metallurgical evaluations, mechanical property tests were conducted to verify the effectiveness of the gas cup unit concept and other possible monitoring and control procedures.

3.2 Materials

The base metal used in this project is a ASTM A36 steel which is 1/2" and 3/4" in thickness. The flux-cored arc welding wires used are:

Innershield NR-204-H (AWS A5.20-79 and ASME SFA-5.20, 0.068");
SOS 308L (1/16");
Russian wire (1/16").

Chemical compositions of the weld deposit of the NR-204-H wire, SOS 308L and weld metal of the Russian wire are shown in Tables 1 and 2.

3.3 Experimental Setup

3.3.1 Underwater Welding Tank

The experimental tests were conducted in the newly established water tank. The tank is constructed of carbon steel and is painted with a marine environment paint. A Plexiglas window is located on the front panel for viewing of the tank interior. Water fills the tank through an inlet which is centered on the lower left end on the tank. A ball valve is located at this point to allow for control of the water flow.

Two independently used outlets are located on the tank for water drainage. The first is used to prevent the water from clouding visibility. During the welding process, water flows continually through the inlet and particles generated from

welding are removed from the top surface. The second outlet is on the bottom of the tank on the right side. This outlet is used for complete drainage of the tank. A shut off valve allows for the tank to be easily drained. Both water outlets are connected and the common lead transports water to the drain. Schematic of the underwater welding tank is shown in Figure 1.

3.3.2 Welding System

The welding system constructed in this project included a constant voltage welding power supply, an automatic wire feeder, a side beam, a travel speed control unit and a fume exhaust system. The control of the side beam motor and the welding power supply was done by adding a double pole single throw switch into the control circuit. This switch allows the operator to turn on the travel control of the side beam and the welding power supply trigger all in one motion. Simplified circuit schematic is shown in Figure 2.

With this type of circuit, the side beam motor control without welding power supply control can still be performed with the original switch. The new switch bypasses the original control switch by running paralleled wires from the contacts of the original switch and connecting these wires into the contacts of the new switch. Only one switch should be turned on at a time. The whole underwater welding system for this project is shown in Figures 3 and 4. Details of the control units on the welding machine, wire feeder and the side beam is shown in Figure 5.

3.4 Welding Tests

The welding test was done both in open air and underwater with and without the addition of the gas cup unit and shielding gas. In order to determine the working range of the parameters, a series of welding tests were carried out using different wires. A choice had to be made regarding the shielding gas. There were several choices: argon, CO_2 and air. The selection of the shielding gas was based on the weld quality criteria and economic issue. After a series of experimental tests, compressed air was chosen as the shielding gas for underwater welding, and the welding parameters used for the evaluation of the welds are set as follows:

Arc voltage: See Tables 4 through 6
Welding current: See Tables 4 through 6
Travel speed: 10"/min.
Polarity: electrode positive
Electrical stickout : 3/4"
Shielding gas: compressed air
Water temperature: 15°C
Water depth: 8"

3.5 Assessment and Evaluation

3.5.1 Visual Examination

After the completion of the weld plates, visual examinations of the welds were conducted based on ANSI/AWS D3.6-93[9] specifications before further evaluations were done.

3.5.2 Chemical Analysis

Chemical compositions of the ferritic steel welds(Russian wire) and the austenitic staniless steel welds (Stoody wire) were analyzed using the Arc Spectra Analysis method and EDS(Energy Dispersive Spectrometry). The sampling sites were in the center part of each weld.

3.5.3 Metallurgical Evaluation

Metallographic sections were cut from typical welded plates, transverse to the welding direction. Mechanical polishing technique was used followed by immersion in enchants. For the ferritic steel welds, a 2% nital solution was used, for the austenitic stainless steel welds, a locally developed etchant consisting of a mixture of the following chemicals were used: methyl alcohol, acetic acid, hydrochloric acid, nitric acid, glycerin and hydrogen peroxide.

3.5.4 Mechanical Property Test

All weld metal tensile(round), reduced section tensile(flat) and side bend tests were conducted on the weld plates. Those

specimens were prepared and tested in accordance with ANSI/AWS D3.6-93[9] and ASTM A370[39] specifications as applicable.

3.5.4.1 All Weld Metal Tensile Test

Dimensions and sampling of the all weld metal tensile test plates are shown in Figure 6. The gage length of the specimens was 2 inches.

3.5.4.2 Reduced Section Tensile Test

Dimensions and sampling of the reduced section tensile test plates are shown in Figure 7. The gage length of the specimens was 2 inches.

3.5.4.3 Side Bend Test

Dimensions and sampling of the side bend test plates are also shown in Figure 7. The thickness of the specimens was 3/9 inches.

3.5.5 Fracture Analysis

Fracture analysis of the welds were conducted using the Scanning Electron Microscopy(SEM) technology. An visual observation of the fracture surface was done before the SEM analysis.

4.0 Design of Welding Gun

In order to eliminate the human factors and find the operational range of different welding materials efficiently, an automatic welding gun was chosen for this period of test. In the next stage, a semi-automatic welding gun will be used.

4.1 Waterproof of Welding Gun

The welding gun used for this project is a modified Miller GA-50A GMAW automatic gun. Modifications to the gun assembly were made so that the inner torch could be protected from water. The addition of o-ring gaskets placed at the bottom of the head tube and within the nozzle extension (See Figure 8) were all that was needed to seal off the main gun body. The inner and outer diameters of the torch and nozzle extension were not standard o-ring splicing kit. The only area left to waterproof was the contact tip and contact tip adapter (See Figure 9). This was done by the use of an o-ring at the top of the contact tip adapter and allen screw plugs in the holes where the gas would usually come out. The o-ring at the top of the adapter seats into the lead tube. The gas expulsion holes were threaded and the allen screw studs were placed into them along with Teflon tape(The use of silicon epoxy may have to be substituted for the Teflon tape). This was done to guard against water leaking into the wire sheath and wetting the flux.

The next step for the modification of the welding gun is the development of a contact tip hole that will seal the wire from the water at all times. There are some conceptual ideas but nothing very conclusive on how this will be accomplished.

4.2 Development of Gas Cup Unit

A gas cup unit(made of bronze) was developed during the first year of this project, as shown in Figures 10 and 11. The two pieces of metal cups are made of bronze which will not suffer from corrosion problems when underwater welding is done. The layer between the two bronze cups is a piece of foam, gases can pass through this layer slowly and uniformly. With the addition of the gas cup assembly, the bubble around the welding arc can grow bigger, and the individual dynamic bubbles escape slower than they do when welding without the gas cup assembly. The whole gas cup assembly makes the shielding gas and the gas from the

bubble escape finely, which results in a more stable arc, and the narrow weld bead caused by the nonuniform change of the dynamic bubble can thus be avoided.

4.3 Embedment of Thermal Couples

The addition of a thermocouple embedded in the side wall of the weld nozzle was studied. The original signal for the feed-back control system will be the temperature inside the dynamic bubble. Another set of gas cup unit was prepared (made of plastics) for the mounting of thermal couple in the unit. With the introduction of thermal couple (alumina-chromi thermal couple at this time), the average temperature inside the dynamic_bubble can be monitored, which will be used for the feed back control (basically welding current control) of the underwater FCAW process.

4.4 Design of The Gas Blanket

The original design of the air blanket is shown in Figure 12(See section A), later this design was modified as shown in Figure 13, the alignment of the slits instead of the nozzles aimed at more efficient utilization of the air and better shielding effect of the weld zone within critical temperatures.

5.0 RESULTS AND DISCUSSION

5.1 Performance of Different Electrodes

The arc stability, bead appearance and weld contour of different electrodes under different welding conditions were evaluated. Welding parameters and weld bead summary for different electrodes tested in air and underwater are shown in Tables 4 through 6. Details of the bead appearance of those welds are shown in Figures 14 through 18.

During the welding tests it was observed that the Russian wire and the SOS 308L wire have good operational properties, such as very little spatter and very fine weld ripples. According to the test results and observations during the air and underwater welding processes, Russian(ferritic) and Stoody(austenitic) wires were chosen for the further evaluation of the smart welding process.

It is also found that for underwater wet welding, a higher heat input, more precisely a higher arc voltage level is needed to achieve a weld with acceptable bead appearance, weld contour and weld properties. This may be caused by two factors, the fast cooling rate and the lower wettability of the liquid metal on the surface of the base metal in a water environment. The addition of some kind of materials in the flux of the wire may improve the wettability of the liquid metal on surface of the base metal in a water environment.

5.2 Effect of the Gas Cup Unit on Performance of Different Electrodes

Figures 19 through 24 show the weld contour of the Russian electrode and the 308L stainless steel electrode tested in air and underwater with and without the addition of the gas cup unit. From these test results, it can be found that it is the addition of the gas cup unit and the shielding gas that makes the improvement of the performance of the electrodes tested underwater. The reinforcement of the wet welds is much lower than those of the wet welds without the addition of gas cup unit. Penetration is greatest when no gas cup unit and shielding gas is used. The good weld contour of the underwater welds with the addition of the gas cup unit will definitely contribute to the

improvement of the fatigue strength of the weldment made underwater.

Based on the test results, the gas cup unit can affect the performance of electrodes underwater by the following ways: (1) weld contour; (2) bead appearance; (3) ductility of the wet welds; (4) tensile toughness of the welds. All of these factors are very important for the application of the underwater wet welding. So far, no open literature is found to report such kind of test results, which may bring the development of underwater wet welding to a much higher level. The idea of the introduction of the gas cup unit is better than other ideas such as creation of semi-dry environment both economically and practically.

5.3 Chemical Compositions of Welds

Chemical compositions of the austenitic stainless steel weld are shown in Tables 6. It can be seen that there is no significant change in the chemistry of the welds made in air and underwater with and without the addition of the gas cup unit. The bulk chemistry of different welds made under different conditions showed the same trend(See Table 7
). From the chemical analysis results, it is expected that the main change in the weld metal microstructure of the stainless steel wire is caused by the solidification modes instead of the change of weld metal chemical compositions.

5.4 Microstructural Features of welds

Figures 25 through 35 show the weld metal and fusion line and heat-affected zone microstructures of the Russian and 308L stainless steel wires tested in air and underwater with and without the addition of gas cup assembly. For the welds of the Russian wire, the microstructures in the weld metal consists of grainboundary ferrite, side plate ferrite and bainite. There is no significant change in microstructures of the air weld and underwater weld in this case. For the welds of the 308L wire, the microstructure in the weld metal is mainly dendritic structure. There are some differences between the microstructure in the air welds and the underwater welds with and without the addition of gas cup unit. Among those welds, the underwater welds with the addition of the gas cup assembly has the smallest partially

mixed zone which may be beneficial for the reduction of the formation of hydrogen-induced cracking in this zone when weld steels with higher carbon equivalent. During the metallurgical evaluation, it was also found that the weld metal of the underwater welds are more sensitive to the etchant than that of the air weld, which may be caused by the different solidification modes in air welds and underwater wet welds.

Neither hydrogen-induced cracking nor solidification cracking was found in the weld metals and the heat-affected zones of the ferritic steel electrodes and the austenitic stainless steel electrode.

5.5 Tensile Properties of Welds

In this section, Tensile strength, tensile ductility(maximum strain to fracture) and tensile toughness of the wet welds will be discussed.

Figure 36 shows all weld metal tensile test samples of different welds. Table 8 shows the tensile test results of different electrodes. Figures 37 through 39 show the stress-strain curves(engineering stress-strain curves) of different welds. It is found that in the case of flux cored arc welding with a gas cup unit, the tensile properties especially the maximum strain to fracture are much better than those welded using shielded metal arc welding electrodes in general. Again, the tensile strength is not a problem for both the ferritic steel weld and the austenitic stainless steel weld. For the austenitic stainless steel weld, the maximum strain to fracture of the underwater wet weld is almost the same as that of the air weld, this can be further proved in the bending ductility session. As the maximum strain to fracture increases, the tensile toughness of the welds also increases(the area under the tensile stress-strain curve). All this kind of information will be very important for the selection of the underwater wet welding materials and processes. It is also indicated that the concept of the gas cup unit is very successful.

5.6 Bending Ductility of Welds

Figures 40 to 41 show side bend test samples of different welds. Table 9 is the side bend test results of different welds. For the austenitic stainless steel weld, one of the bending angle reaches 180°, which indicates an approximately 20% of the ductility of the weld, for underwater wet welding, this is so far the best results according to the open literature. The test results are also in good agreement with the tensile test results. It is thought that the concept of gas cup unit is the key factor contributing to the good ductility of the wet welds prepared by the smart welding process.

5.7 Fracture Morphologies of Welds

Figure 42 shows the fracture analysis results of different welds. Both Figure 42a and b(underwater wet welds)show dominant fibred fracture surfaces, which are a sign of ductile fracture mode. In comparison with the air weld fracture surface(Figure 42c), the fracture surface of the underwater wet welds show subcracks which are thought to be caused by the hydrogen effects of the underwater wet welds. Figure 43 a and b show fisheyes in the fracture surface of the ferritic steel underwater wet welds, and Figure 43c shows quasicleavage fracture mode inside the fisheye, which shows the local hydrogen embrittlement of the underwater wet welds. However, it can be seen that in this case the shapes of the fisheyes are more irregular than the welds made with shielded metal arc welding electrode underwater[21], which means a better ductility and toughness of the former case. Figure 44 shows the dimple fracture mode of different welds, it can be seen that the difference between the fracture mode of the underwater wet welds and the air weld is that there are some tearing ridges in the fracture surface of the air weld instead of the underwater wet welds. This indicates that for underwater wet welds, be it ferritic steel or austenitic stainless steel, the ductility is always worse than those of the corresponding air welds, one of the dominant factor is the hydrogen embrittlement effects. Figure 45 shows subcracks in different underwater wet welds, again, this is a typical hydrogen embrittlement sign. Figure 46 shows both the ductile fracture mode (dimples) and brittle fracture mode(quasicleavage) at the same fracture of the austenitic stainless steel weld.

From the test results in this section, it can be concluded that for all underwater wet welds, hydrogen embrittlement can not be thoroughly avoided, be it ferritic steel weld or austenitic stainless steel weld. However, the extent to hydrogen embrittlement can be reduced by proper shielding effect, as mentioned above, the addition of shielding cup unit.

6.0 CONCLUSIONS

A flux-cored arc welding system was set up and a gas cup unit was developed to improve the quality of underwater wet welds. The effectiveness of the gas cup unit was observed. Main conclusions are summarized as follows:

1. The heat input, especially the arc voltage to get acceptable weld bead appearance and weld contour for the underwater wet welds is higher than that of the air welds. Fast cooling rate and lower wettability of the liquid metal on surface of the base metal in a water environment contribute to this phenomenon.

2. The addition of the gas cup unit can improve the underwater wet welds performance especially the weld contour significantly by making the bubble and the gas within the arc cavity escape slowly and uniformly.

3. There is no significant change in chemical compositions of the air welds and underwater wet welds with and without the addition of the gas cup unit under these test conditions.

4. The change of microstructure of the air weld and the underwater wet welds of the stainless steel wire is expected to be caused by the solidification mode differences instead of the change of chemical compositions. The partially mixed zone in the weld metal of SOS 308L wire with the addition of the gas cup unit is the narrowest in comparison to those of the air weld and underwater wet weld without the addition of the gas cup assembly.

5. The performance of the Russian wire and the SOS 308L wire is better than the Innershield NR-204-H wire under these test conditions .

6. Hydrogen embrittlement of underwater wet welds, including reduction of mechanical properties especially the reduction of ductility and toughness, can be reduced significantly by the FCAW process in this study. The most important idea is the addition of the gas cup unit. With the modification of the utilization of the gas cup unit, further improvement of the underwater wet welds can be expected. This may direct the research and development of underwater wet welding to a new stage.

7.0 Recommendations for Continuity

1. The effects of the gas cup assembly on the performance of different electrodes and the weld properties should be further investigated in order to improve the present gas cup unit.

2. Modification of the Gas Blanket Assembly is necessary for the improvement of wet weld quality.

3. Development of the Feedback Control System

4. Implementation of the Vision System

5. A specific method instead of high speed photography should be developed for the study of dynamic bubble around the welding arc.

6. It is necessary to measure the hydrogen level in the weld metal of the underwater wet welds to verify the effect of shielding gas on the reduction of partial pressure of hydrogen in the arc atmosphere.

8.0 REFERENCES

1. Brown,A.J., Brown,R.T., Tsai,C.L., and Masubuchi,K.1974. Report on fundamental research on underwater welding. Report No. MITSG 74-29.
2. Tsai,C.L., Ozaki,H., Moore,A.P., Zanca,L.M., Prasad,S.,and Masubushi,K. 1977. Development of new, improved tecniques for underwater welding. Report No. MITSG 77-9.
3. Ibarra,S., Grubbs,C.E. and Olson,D.L. 1988. Metallurgical aspects of underwater welding. Journal of Metals. (12),8-10.
4. Sanchez-Oslo, A., Liu,S., and Olson,D.L.1993. Underwater wet welding consumables for offshore applications. Proceedings of the Int'l Conf. on OMAE, ASME, No.G0679A,pp.119-128.
5. Tsai,C.L., 1989. Evaluation design and fabrication methods for underwater welding. Welding Innovation Qauaterly 6(1).
6. Tsai,C.L., Feng,Z.L., Grantham,J., and Soission,L.,1990. Connection Pad Design for Underwater Tubular Structures. Welding Journal,69(1),p.53-57.
7. Tsai,C.L.,Zirker,L., Feng,Z.L., Grantham,J., and Papritan,J.,1991. Fitness-for-service design for underwater "wet" welds, Tenth International Conference on Offshore Mechanics and Arctic Engineering, ASME, Vol.III-A, Materials Engineering. pp.197-204.
8. Tsai,C.L., Jian,L., Grantham,J and Feng, Z.L.1992. Development of flux-coated electrodes for underwater wet welding. Eleventh International Conference on Offshore Mechanics and Arctic Engineering, ASME,92-841M.
9. ANSI/AWS D3.6-93. American Welding Society.
10. Draugelates,U.,Bouaifi,B.,andBartzsch,J.1994. Investigations on local shielding systems for underwater applications. Proceedings of the Fourth International Offshore and Polar Engineering Conference. pp.120-129.
11. Song,B.T.1994. Development of underwater welding and cutting technologies in China.
12. Watson,P.D., Dexter,R.J. and Shick,W.R. 1990. Underwater welding, a ;iterature search.SwRI Project No. 06-2472, prepared for a consortium of Oil and Gas Companies.
13. Hamann,R., and Mahrenholtz,O. 1994. On the influence of the surface heat transfer coefficient on wet underwater welding. Proceedings of the fourth international offshore and polar engineering conference. PP.112-119.
14. Avilov,T.I., 1960. Peroperties of underwater arcs.Weld Prod.

7(2). p30-33.
15. Ibarra,S., Olson,D.L.and Liu,S. 1992. Effect of water depth on underwater weld metal porosity formation. International Conference on Underwater Welding: AWS,pp.54-69.
16. Dexter,R.J., Norris,E.B., Schick, W.R., and Watson,P.D.1986. Performance of underwater weldments. Final report on contract DTCG23-82-C-20017, Report No. SSC-335, Ship Structure Committee.
17. Ogden,D. and Joos,T. 1990. Specification stirs underwater electrode development. Welding Journal, 69(8).
18. West,T.C.,Mitchell,G and Lindberg,E. 1990. Wet welding electrode development. Welding Journal, 69(8).
19. Garland,J.G. and Bailey,N. 1975. Welding Research International. 5(3), P1-33.
20. Maddox, S.J. 1970. Proceedings of 'Fatigue of welded structures' Conference. The Welding Institute. p73-96.
21. Tsai,C.L., Jiang,C.H., Hall,S. and Zhou,M.H.1994. Verification and dissemination of the required engineering data base for the new underwater, flux-coated welding electrode in commercial applications. Annual Report submitted to the National Coastal Resources Research and Development Institute.
22. Shannon,G.J., Watson,J and Deans,W.F. 1994. Investigation into the underwater laser welding of steel. Journal of Laser Applications. 6, p223-229.
23. Blakemore,G.R.1993. Friction stud welding in hazardour areas. Welding and metal fabrication.61(9),Nov-Dec.
24. dos Santos,V.R., Teixeira,J.C.and dos Santos,J.F. 1993. Qualification trials of the "MOSS" modular orbital welding system.Proceedings of the Third International Offshore and Polar Engineering Conference. p434-440.
25. McMaster,R.S., Nixon,J.H., Boyle,B.G. and Fouchier,D. 1994. Task Enhancement of an Underwater Robotic Arm by Graphical Simulation Techniques. Proceedings of the 1994 IEEE Oceans Congerence. Part(2), P163-167.
26. Avilov,G.I. 1955. The experience of underwater argon arc welding application. Weld. Prod. No.8.
27. Savich,I.M. 1969. Underwater flux-cored welding. auto. weld. No.10.
28. Grubbs,C.E. and Seth,O.W. 1976. Underwater wet welding with manual metal arc electrodes. Presented at the International Underwater Welding Seminar, London.
29. Grubbs,C.E. 1986. Qualification of underwater wet welding procedures at water depths down to 325 feet. International

Diving Symposium, Houston, Texas.
30. Cochrane,D.J., Swetnam,D. 1986. Wet welding-a viable technique? Metal Construction, 18(11).
31. Matlock,D., Edwards,G., Olson,D. and Ibarra,S. Effect of sea water on the fatigue crack propagation characteristics of welds for offshore structures. Journal of Materials Engineering, 9(1).
32. Stakler,A.,Hart,P., and Salter,G. 1975. An assessment pf SMA electrodes for underwater welding of C-Mn structural steel. OTC PaperNo.2301.
33. Tsai,C.L., Jiang,C.H., Hall,S.,Yao,P.L., Svekric,W.A., Holdren,R.L.and Wilsoncroft,C.B. 1995. Engineering assessment of weld joint design for underwater "wet" welding. Final Report submitted to the Navy Joining Center.
34. The Navy Joining Center, 1995. Underwater Wet Welding Reduces Ship Maintenance Costs. Feature Article. Welding Journal, 74(10), 90.
35. Chew,B. 1973. Prediction of weld metal hydrogen levels obtained under test conditions. Welding Journal, 52, 386s-391s.
36. Gretskii,Yu.A., Maksimov,S.Yu. and Kravchenko,N.V. 1993. Effect of marble in rutile electrode coating on the hydrogen content in weld metal in underwater welding. Avtom.Svarka. (7), 51-52.
37. Suga,Y. 1990. The effect of cooling rate on mechanical properties of underwater wet welds in gravity arc welding. Transactions of the Japan Welding Society. 21(2).
38. Hutt,G., West,A. and Starsmore,R. 1995. Hot tapping on a subsea pipeline. Welding and Metal Fabrication. April. p136,138-139.
39. ASTM A370, American Society of Mechanical Engineers.

Table 1 Chemical compositions of the weld deposit of the NR-204-H and SOS 308L wires*

	C	Mn	Si	Cr	Ni	Mo	S	P	Cu	Al
NR-204-H	0.175	1.14	0.18	-	-	-	0.006	0.019	-	0.72
SOS 308L	0.026	1.28	0.41	20.12	9.4	0.2	0.01	0.03	0.1	-

* From air welds

Table 2 Chemical Composition of the Russian wire weld metal with different steels[38]

Steel grade	Analyzed zone	Element wt%							
		C	Si	Mn	Ni	Cr	Cu	S	P
09Г2	BM	0.13	0.4	1.4	0.03	0.05	0.12	0.014	0.026
	WM	0.03	0.03	0.15	1.4	0.03	0.08	0.019	0.025
10ХСН	BM	0.08	0.65	0.53	0.57	0.59	0.36	0.032	0.024
	WM	0.02	0.02	0.09	1.65	0.08	0.12	0.021	0.017
A36	BM	0.2	0.22	0.97	0.05	_	_	0.012	0.014
	WM	0.02	0.03	0.11	1.5	_	_	0.023	0.013

Table 3 Welding parameters and weld bead summary for innershield NR-204-H electrode

Code	Arc Characteristics				Bead Appearance	Defect
	Amperage(A)	Voltage(V)	Heat Input (J/mm)	Stability		
L1-1	170--180	22	908.6	Fair	Good	None
L1-2	100--200	22	778.8	Poor		
L2-1	180--190	22	960.5	Fair	Good	High reinforcement
L2-2	100--200	22	778.8			
L3-1	170--180	24	991.2	Good	Good	None
L3-2	200-210	24	1161.1	Fair	Fair	Ununiform weld,crater porosity
L4-1	180--190	24	1047.8	Good	Good	None
L4-2	220--230	24	1274.4	Poor	Poor	Ununiform weld,crater porosity
L5-1	200--210	24	1164.1	Fair	Good	None
L5-2	200--260	24	1302.7			
L6-1	200--210	26	1257.9	Good	Good	Porosity
L6-2	240--250	26	1503.3	Good	Fair	Unflat crater
L7-2	240--250	28	1618.9	Good	Fair	Unflat crater
L8-1	270-280	30	1947.0	Good	Fair	Surface porosity
L8-2	300-320	30	2194.8	Good	Poor	crater blast
L9-1	280-300	30	2053.2	Good	Fair	Surface porosity
L9-2	320-340	30	2336.4	Good	Poor	Crater blast

Note: -1 : Air welding ; -2: Underwater welding

Table 3 : Continued

Code	Arc Characteristics				Bead Appearence	Defect
	Amperage(A)	Voltage(V)	Heat Input	Stability		
L10-1	260-270	28	1751.1	Good	Good	
L11-2	300--360	24	1869.1			
L12-2	280--300	24	1642.6	Poor	Poor	
L13-2	260--280	24	1529.3	Fair	Poor	
L14-2	240--260	24	1416.0	Fair	Fair	
L15-2	220--240	24	1302.7	Fair	Good	
L16-2	200--210	24	1161.1	Fair	Good	
L17-2	220--240	26	1411.3	Fair	Good	
L18-2	200--210	26	1257.9	Good	Good	
L19-2	160--170	22	856.7	Poor	Poor	
L20-2	140-160	22	778.8	Poor	Poor	

Note:

-1: Air welding ;

-2 :Underwater welding

Table 4 Welding parameters and weld bead summary for SOS 308L electrode

Code	Arc Characteristics				Bead Appearance
	Amperage(A)	Voltage(V)	Heat Input (J/mm)	Stability	
S 1-1	80--90	24	481.4	Poor	Poor
S 1-2	190--200	28	1288.6	Good	Poor
S 2-1	90--100	24	538.1	Fair	Poor
S 2-2	170--180	28	1156.4	Good	Poor
S 3-1	90--100	26	582.9	Good	Fair
S 3-2	180-190	28	1222.5	Good	Poor
S 4-1	90--100	28	627.8	Good	Fair
S 4-2	90--100	28	627.8	Fair	Fair
S 5-1	100--110	26	644.3	Good	Good
S 5-2	100--110	26	644.3	Fair	Poor
S 6-1	130--140	28	892.1	Good	Good
S 6-2	130--140	28	892.1	Fair	Poor
S 7-1	170--180	28	1156.4	Good	Good
S 7-2	170--180	28	1156.4	Good	Poor
S 8-2	190	28	1255.5	Good	Poor
S 8-3	190	28	1255.5	Good	Poor
S 9-2	180	27	1146.9	Good	Poor
S 9-3	180	27	1146.9	Good	Poor

Note: -1: Air welding ; -2 Underwater welding; -3 Underwater welding with gas gun

Table 5 Welding parameters and weld bead summary for Russian electrode

Code	Arc Characteristics			Bead Appearance
	Amperage(A)	Voltage(V)	Heat Input (J/mm)	
A 1-2	150--160	20	731.6	Poor
A 2-2	150--160	22	804.8	Poor
A 3-2	150--160	24	877.9	Poor
A 4-2	150--160	21	768.2	Fair
A 5-2	150--160	26	955.1	Fair
A 6-2	150-160	28	1024.2	Fair
A 7-2	180--190	28	1222.5	Good

Note : -1 : Air welding ; -2 Underwater welding ;

Table 6 Chemical compositions of the SOS 308L welds*(wt%)

	Fe	Cr	Mn	Ni
Air weld	76.56	15.04	1.36	6.76
	77.73	14.62	1.24	6.21
	76.28	15.10	1.39	7.04
	77.49	14.80	1.27	6.36
	76.94	15.31	1.31	6.23
Underwater weld	73.92	16.74	1.22	7.54
	74.05	16.80	1.17	7.55
	73.85	16.71	1.28	7.68
	74.17	16.46	1.38	7.51
	74.58	16.48	1.29	7.35
Underwater weld (with gas cup set)	75.77	14.05	1.31	7.56
	7.27	15.85	1.06	5.67
	75.83	15.35	1.31	7.45
	76.74	14.96	1.30	6.89
	75.75	15.51	1.33	6.62

* by EDS, in weld center parts.

Table7 Weld Metal Chemical Compositions of Different Electrodes(1/16"), wt%

	C	Mn	P	S	Si	Cu	Sn	Ni	Cr	Mo	Al	V	Nb	Zr	Ti	B	Co
Ferritic steel (Russian wire, 1ffw)	<0.01	<0.1	0.016	0.019	<0.01	0.033	0.003	1.6	0.025	0.008	<0.01	0.002	0.001	0.002	0.003	0.0000	0.005
Austenitic stainless steel (Stoody wire, 1ffw)	0.017	1.64	0.029	0.008	0.449	0.155		9.77	20.86	0.16		0.057	0.013				0.127
Austenitic stainless steel (Stoody wire, air weld)	0.018	1.80	0.029	0.007	0.545	0.154		9.68	21.29	0.15		0.062	0.016				0.124

Table 8 All Weld Metal Tensile Test Results of Diffiret Electrodes (1/16")

	Yield strength *ksi*	Ultimate tensile strength *ksi*	% Elongation
Ferritic steel (Russian wire, 1ffw)	56.2	65.8	20.0
Austenitic stainless steel (Stoody wire, 1ffw)	69.7	87.1	25.5
Austenitic stainless steel (Stoody wire, air weld)	69.8	92.8	28.9

Table 9 Reduced Section Tensile Test Results of Different Electrodes(1/16")

	Yield strength *ksi*	Ultimate tensile strength *ksi*	% Elongation	Note
Ferritic steel (Russian wire, 1ffw)	48.8	66.0	8.5	broke in weld metal near fusion boundary
Ferritic steel (Russian wire, 1ffw)	54.5	74.5	14.0	broke in weld metal
Austenitic stainless steel (Stoody wire, 1ffw)	48.4	75.5	8.5	broke in weld metal slag entrapment in fracture surface
Austenitic stainless steel (Stoody wire, 1ffw)	47.4	57.0	8.0	broke in base metal

Table 10 Side Bend Test Results of Different Welds

Electrode	Thickness of the specimen *T, in.*	Die diameter	Bending angle *degree*
Ferritic steel (Russian wire, 1ffw)			
RW1	1/4	2T	Broken
RW2	1/4	4T	Broken
RW3	1/4	4T	35
RW4	1/4	4T	40 (Cracked)
Austenitic stainless steel (Stoody wire, 1ffw)			
SW1	1/4	4T	65
SW2	1/4	4T	40
SW3	1/4	4T	40
SW4	1/4	4T	180

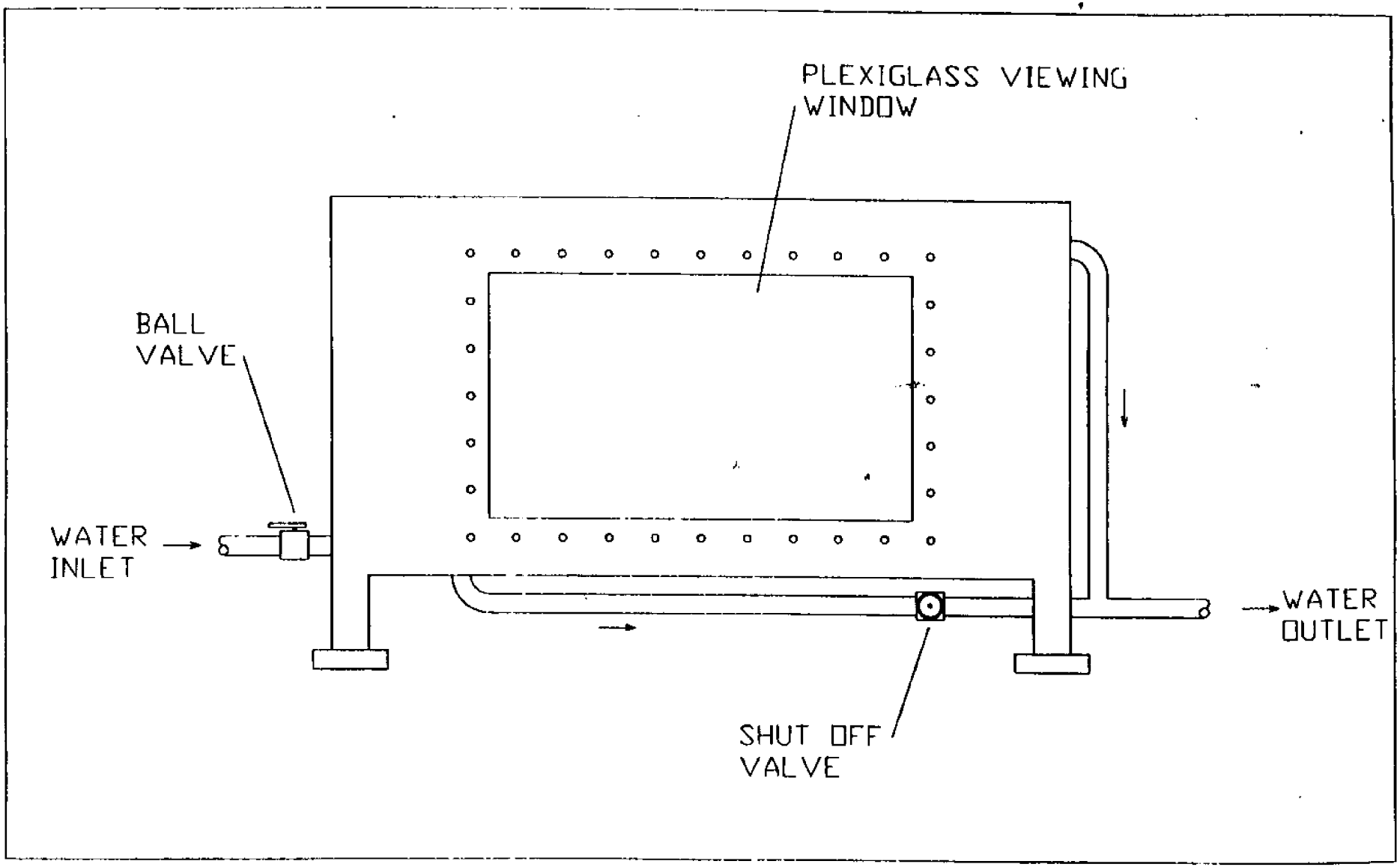

Figure 1 Schematic of the underwater welding tank

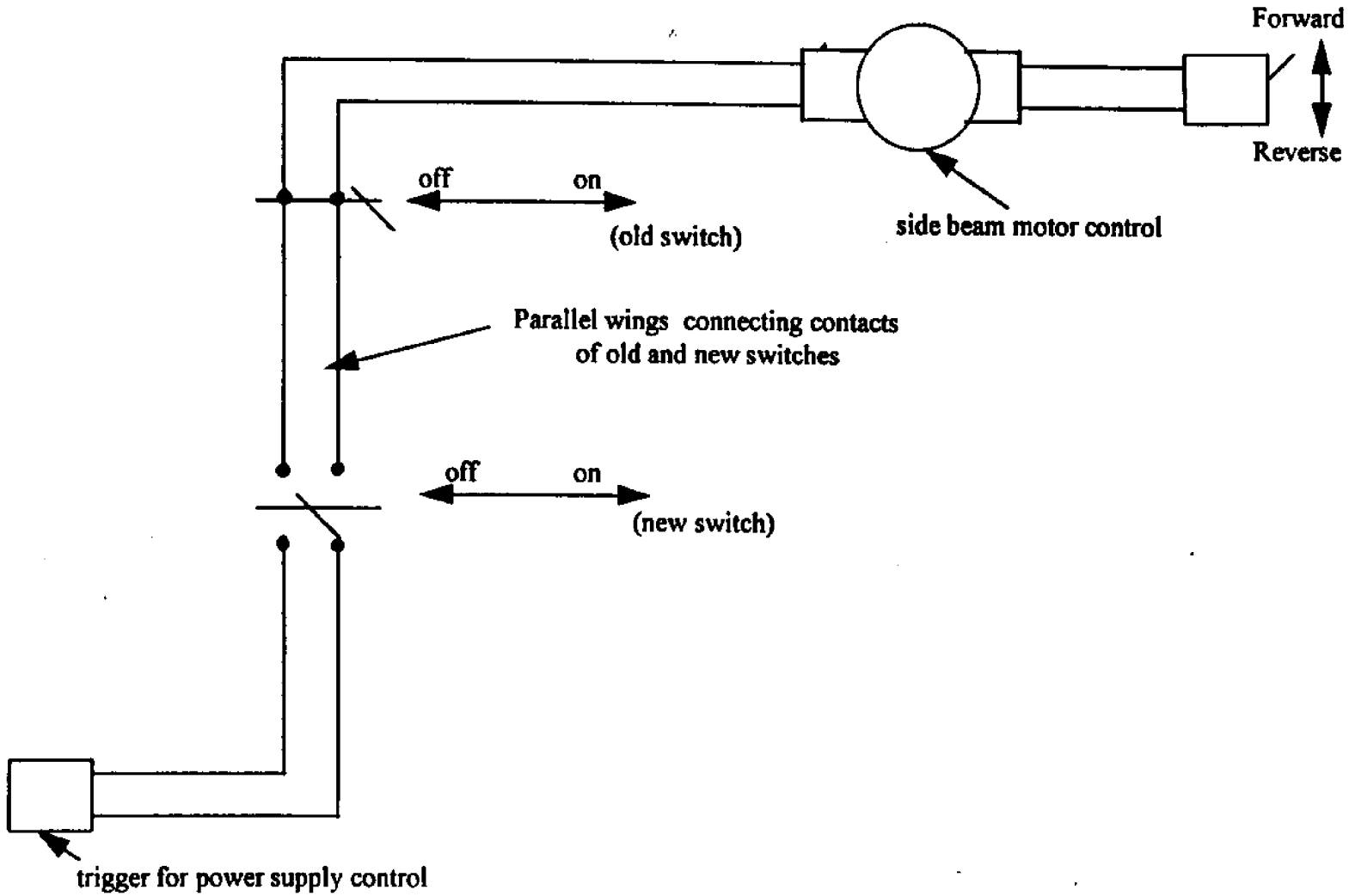

Figure 2 Schematic of the Synchronized Control Circuit

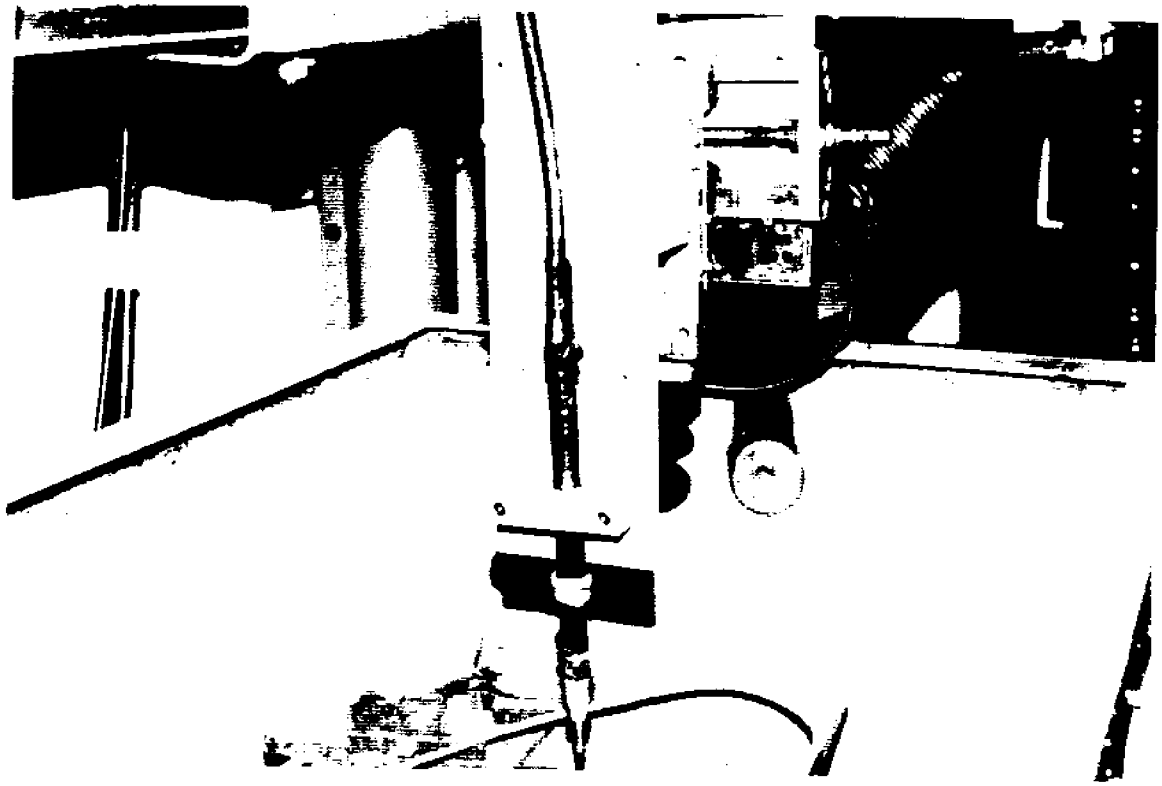

Figure 3 The Underwater Welding System

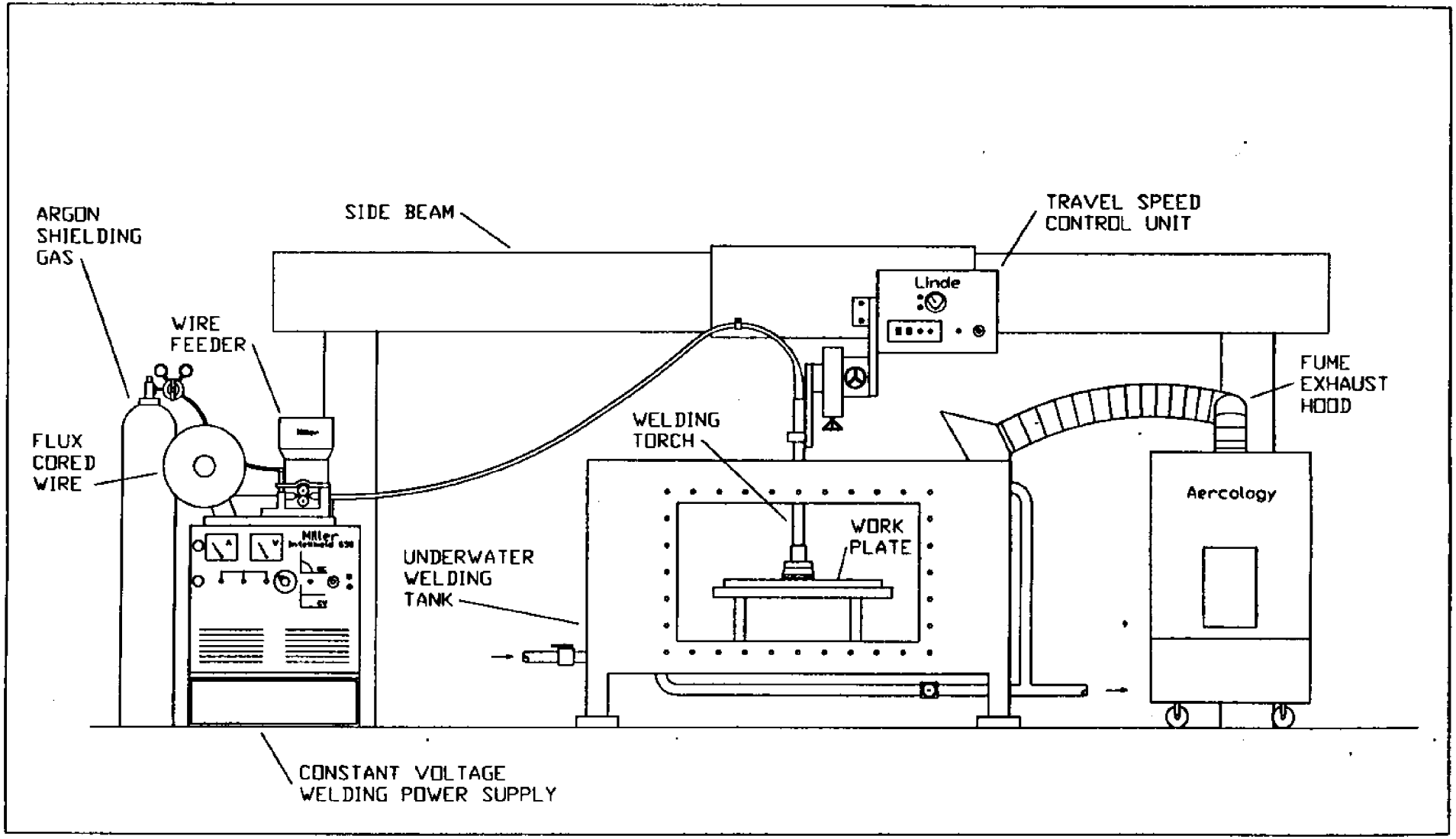

Figure 4 Arrangement of the Underwater Welding System

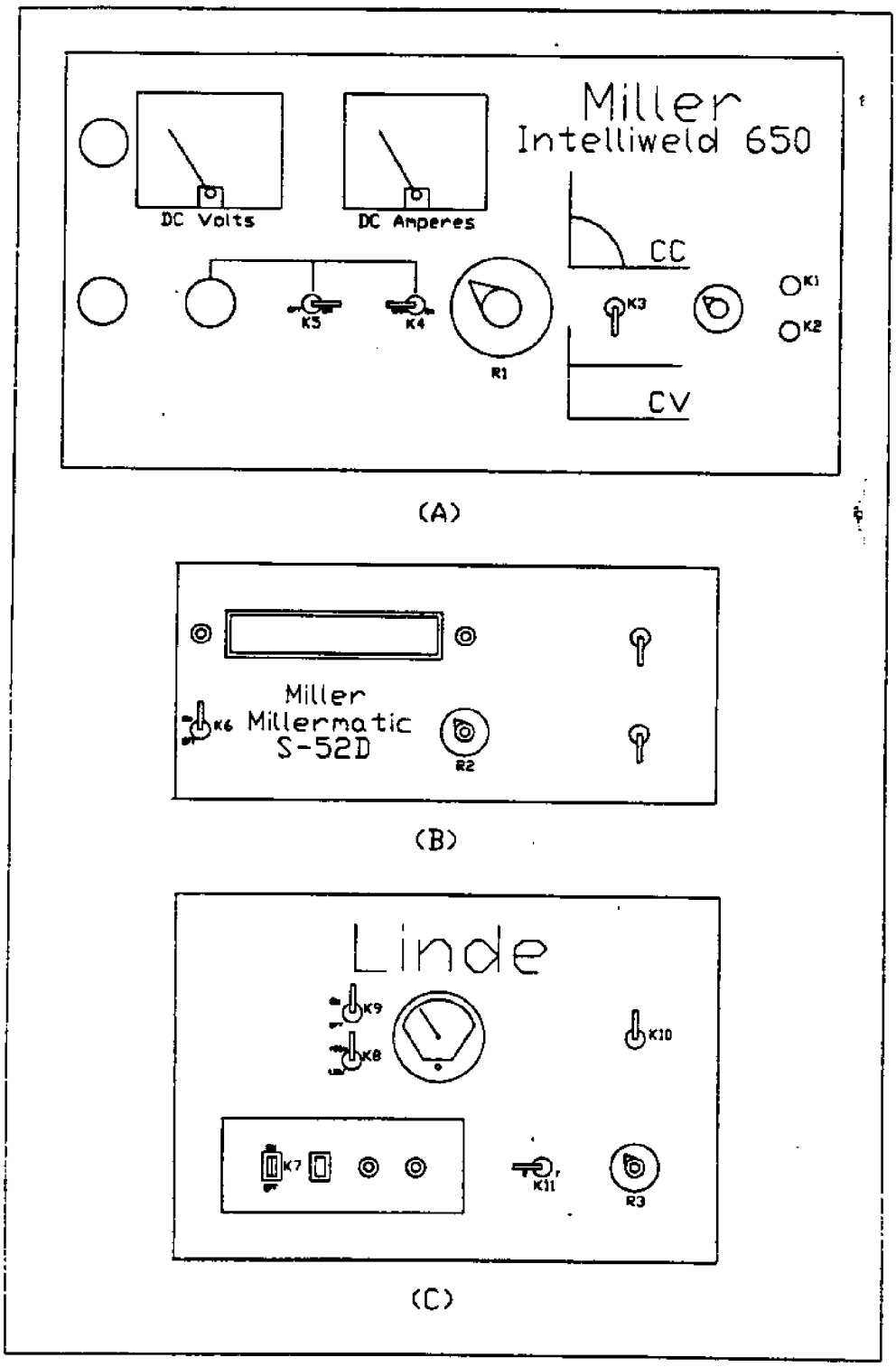

Figure 5 Schematic of the welding control units

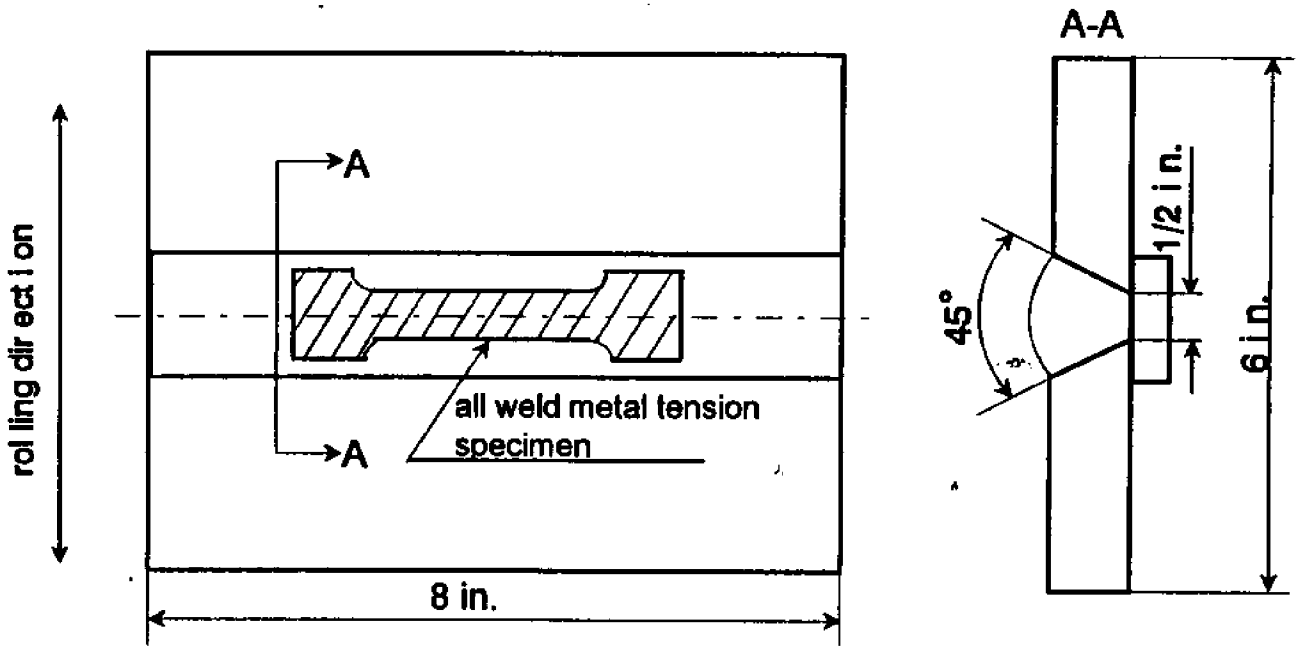

Figure 6 All Weld Metal Tensile Test Plate

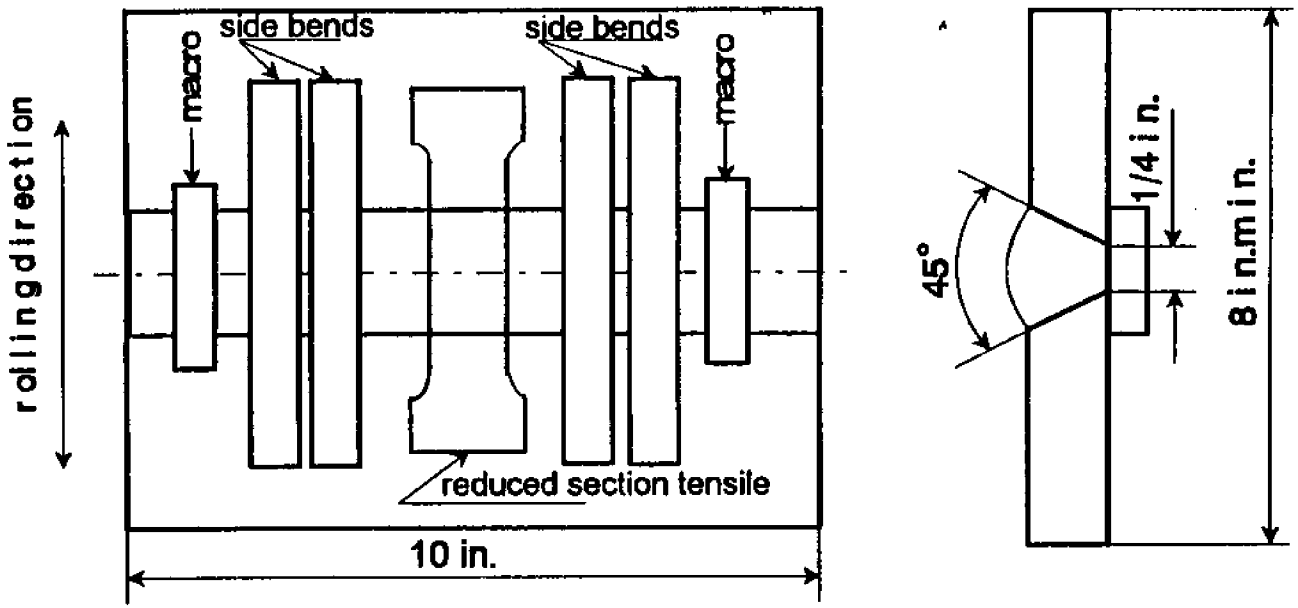

Figure 7 Side Bend and Reduced Section Tensile Test Plate

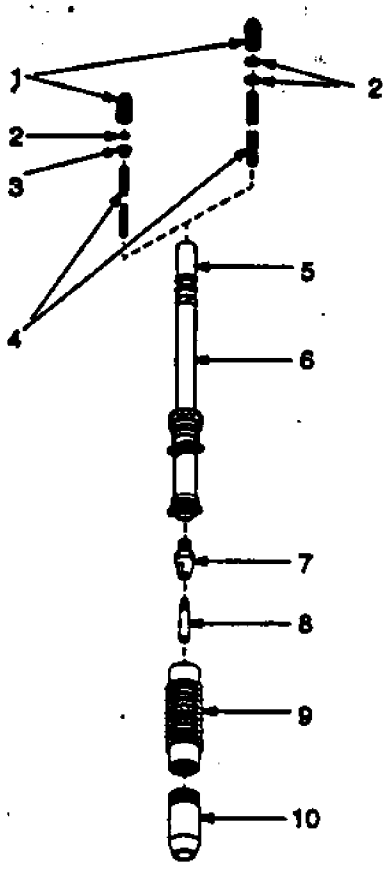

1 Wire Outlet Guide

2 O-Ring

3 Liner Bushing

4 Liner

Remove O-ring and bushing (if present) from liner and install on new liner one inch (25 mm) from end.

5 Gun/Feeder Adapter

6 Head Tube

7 Contact Tip Adapter

8 Contact Tip

9 Nozzle Extension

10 Nozzle

Choose correct parts for wire size, (see Table 5-4) and disassemble gun as necessary to install new parts. Install new parts, and reassemble gun. Reinstall into wire drive assembly.

Figure 8 Waterproof of the Head Tube and Nozzle extension

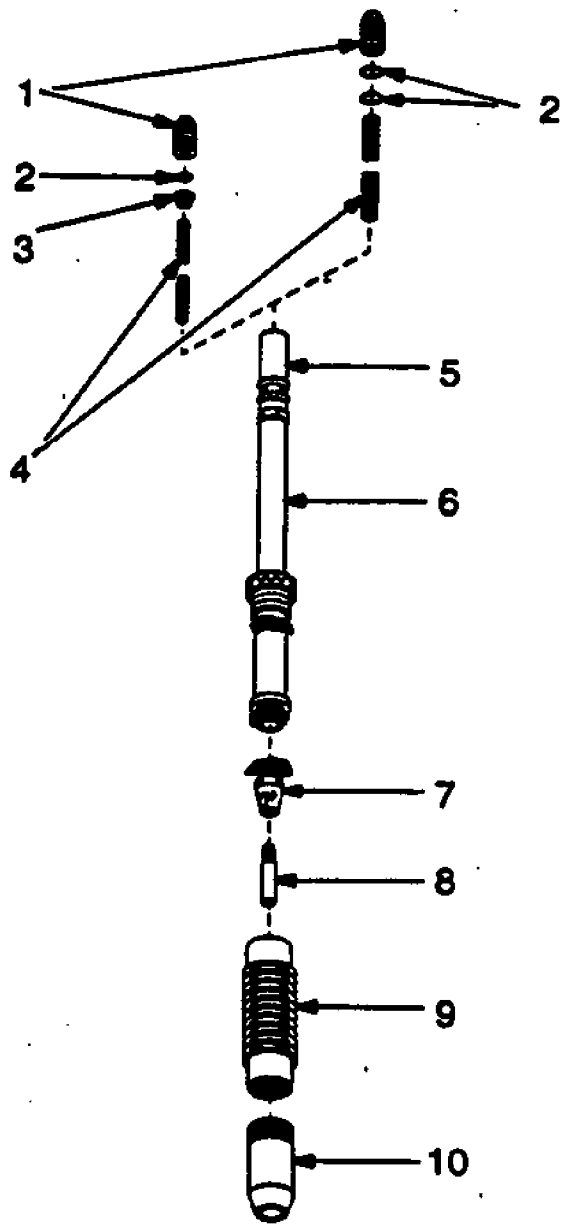

Figure 9 Waterproof of the Contact Tip and Contact Tip Adapter

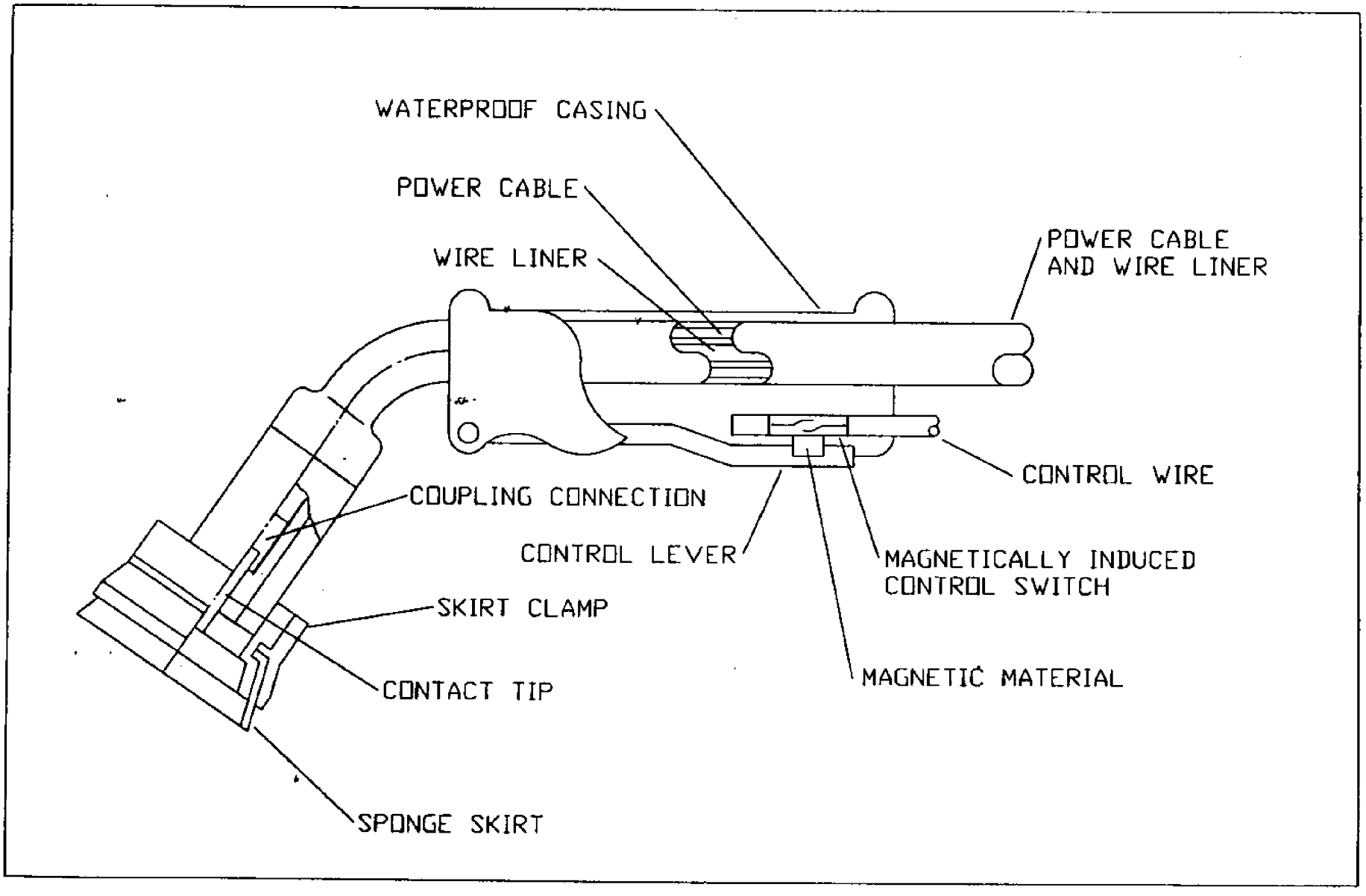

Figure 10 Schematic of the Welding Gun Assembly

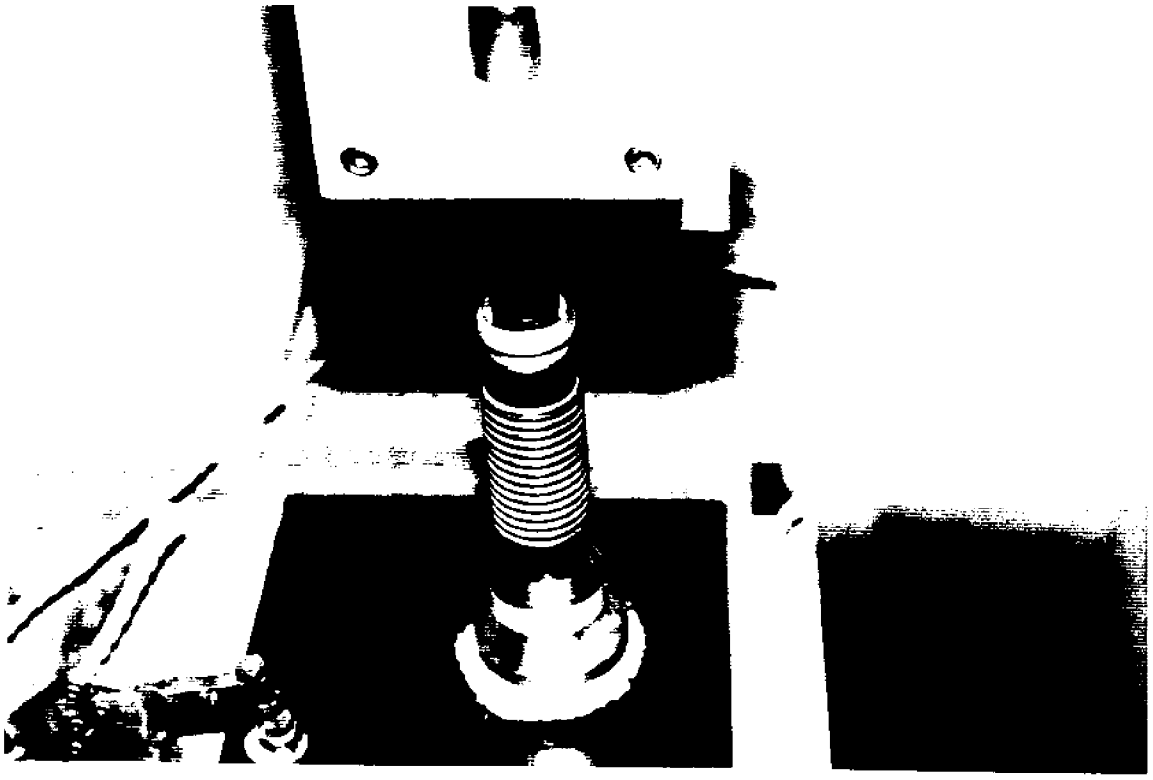

Figure 11 Plans of the Gas Cup Assembly

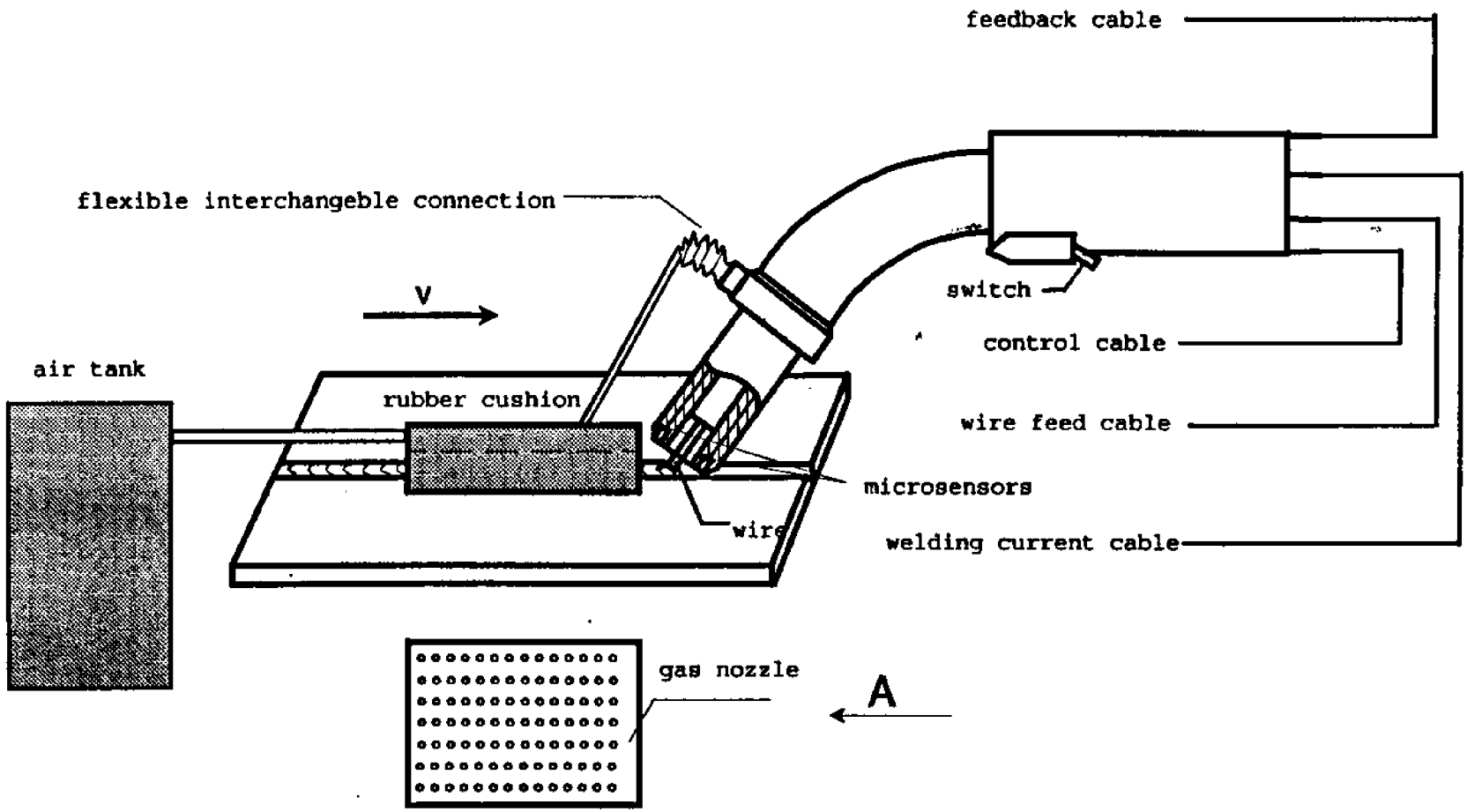

Figure 12 Schematic Diagram of Underwater "Wet" Welding Gun

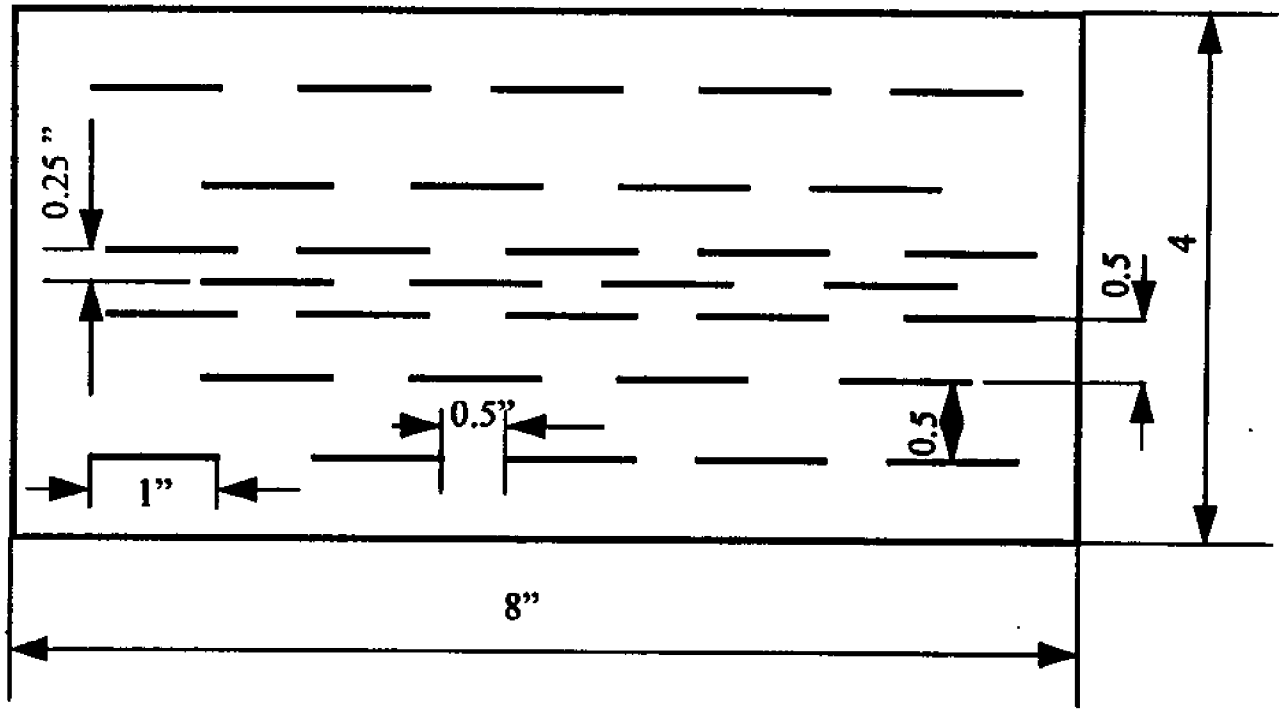

Figure 13 Schematic of the Air Blanket Design

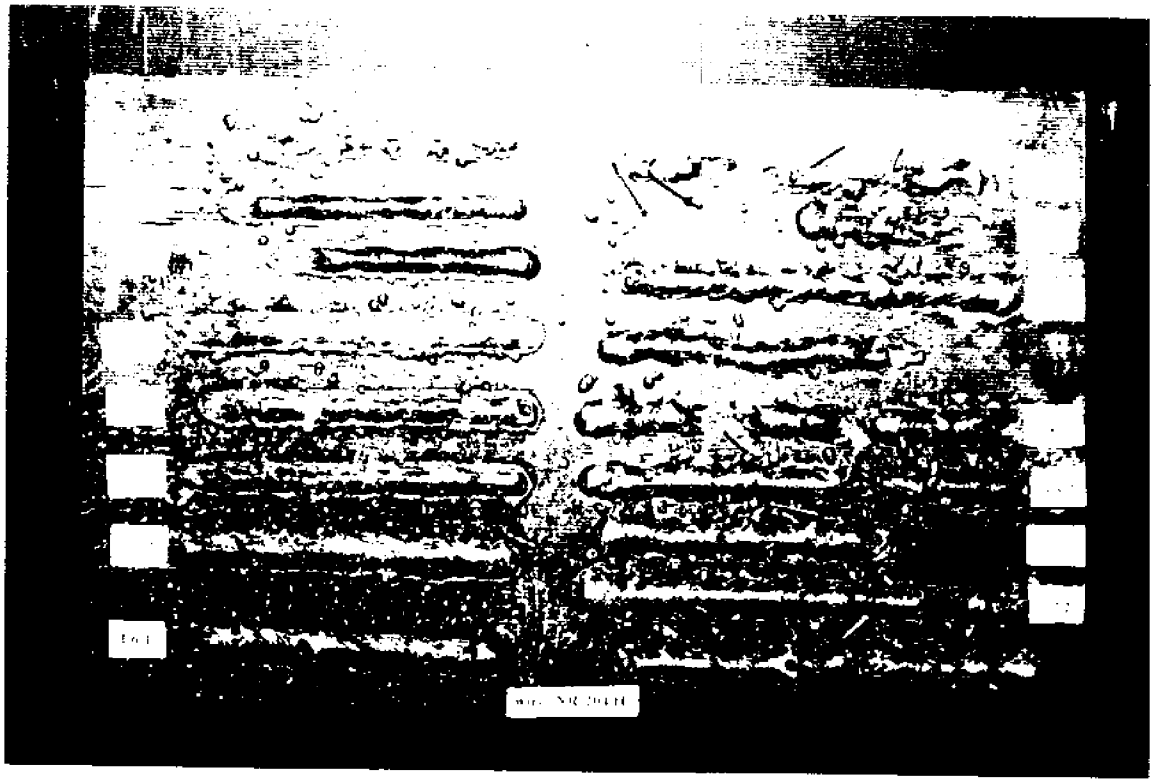

Figure 14 Bead Appearance of the NR-204H Welds

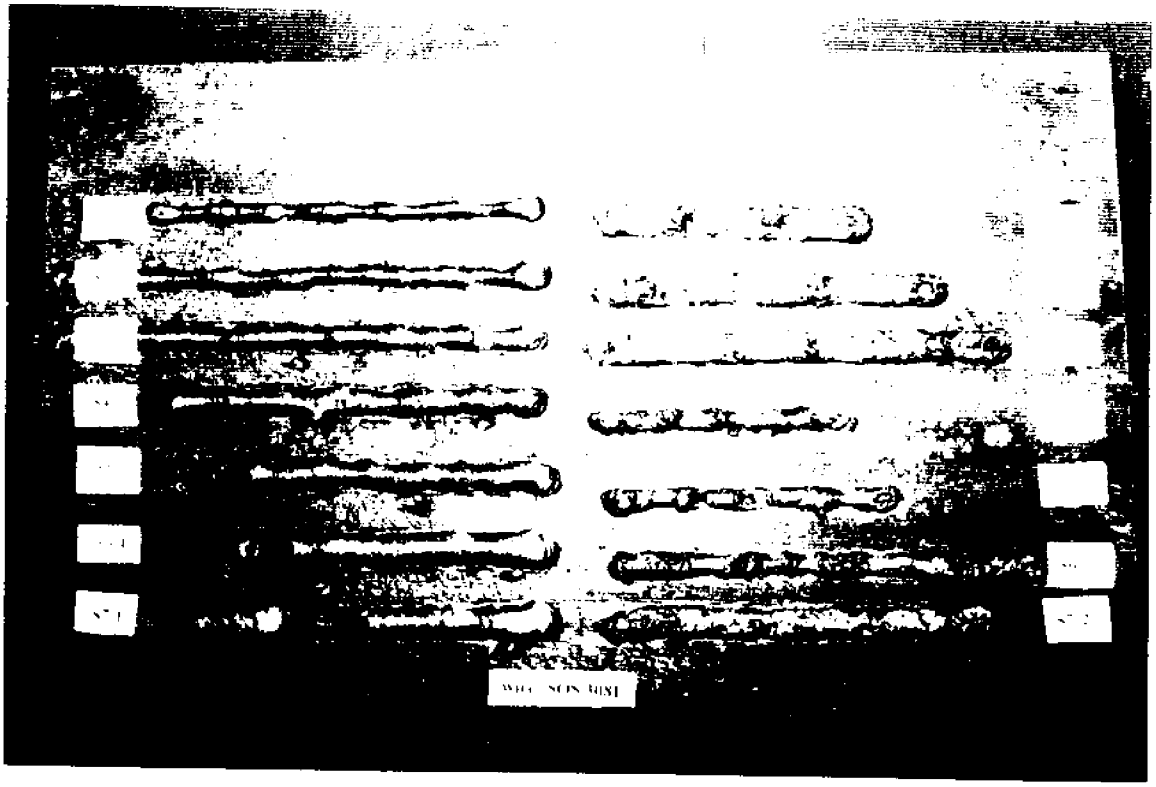

Figure 15 Bead Appearance of the SOS 308L Welds

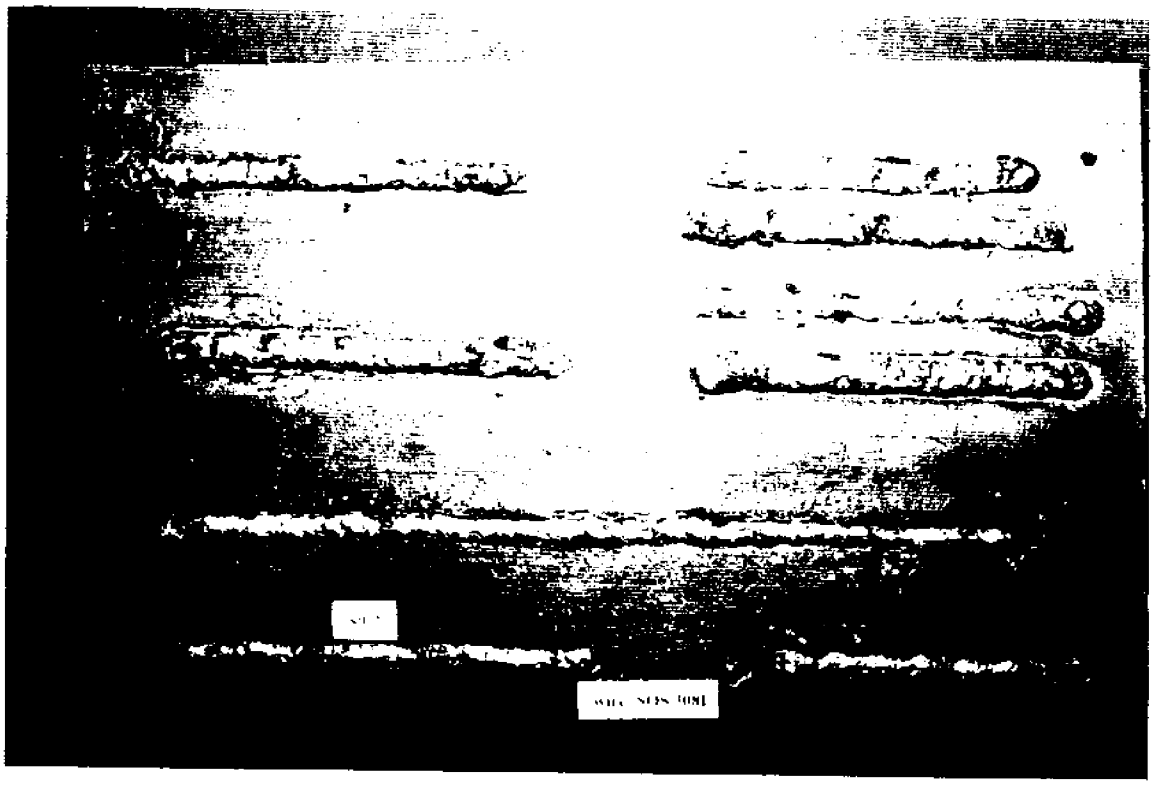

Figure 16 Bead Appearance of the SOS 308L Welds

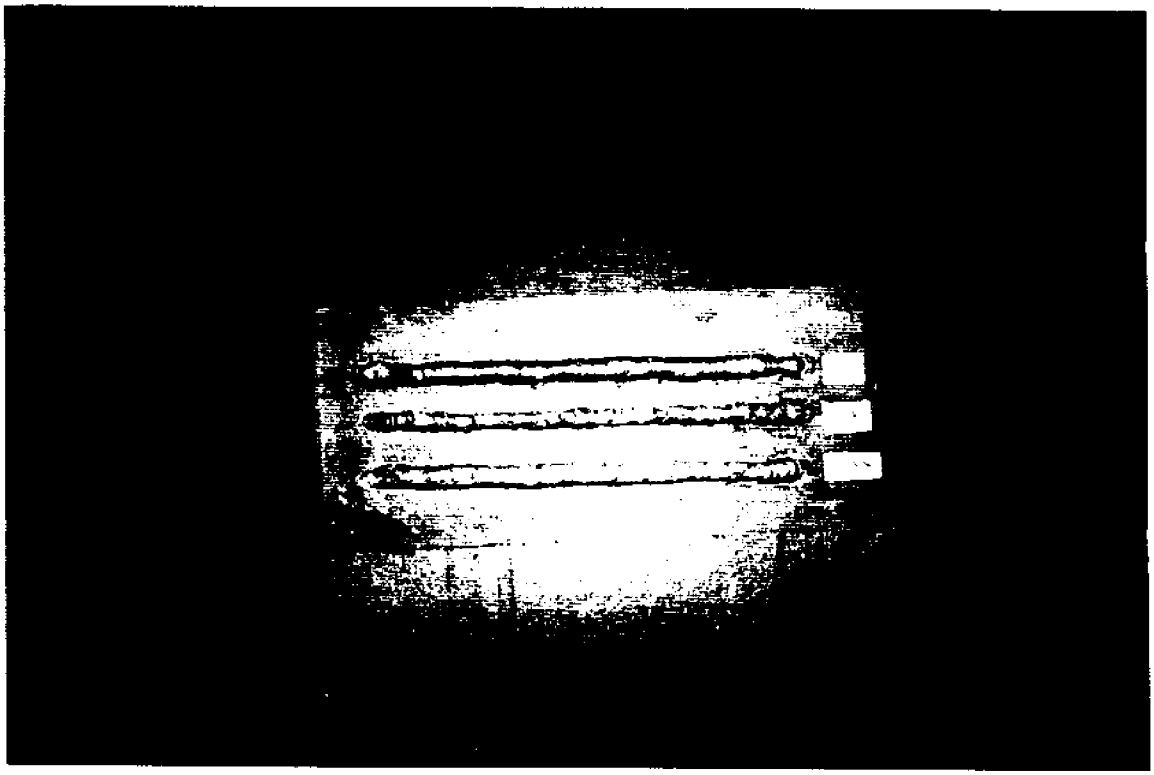

Figure 17 Bead Appearance of the SOS 308L Welds

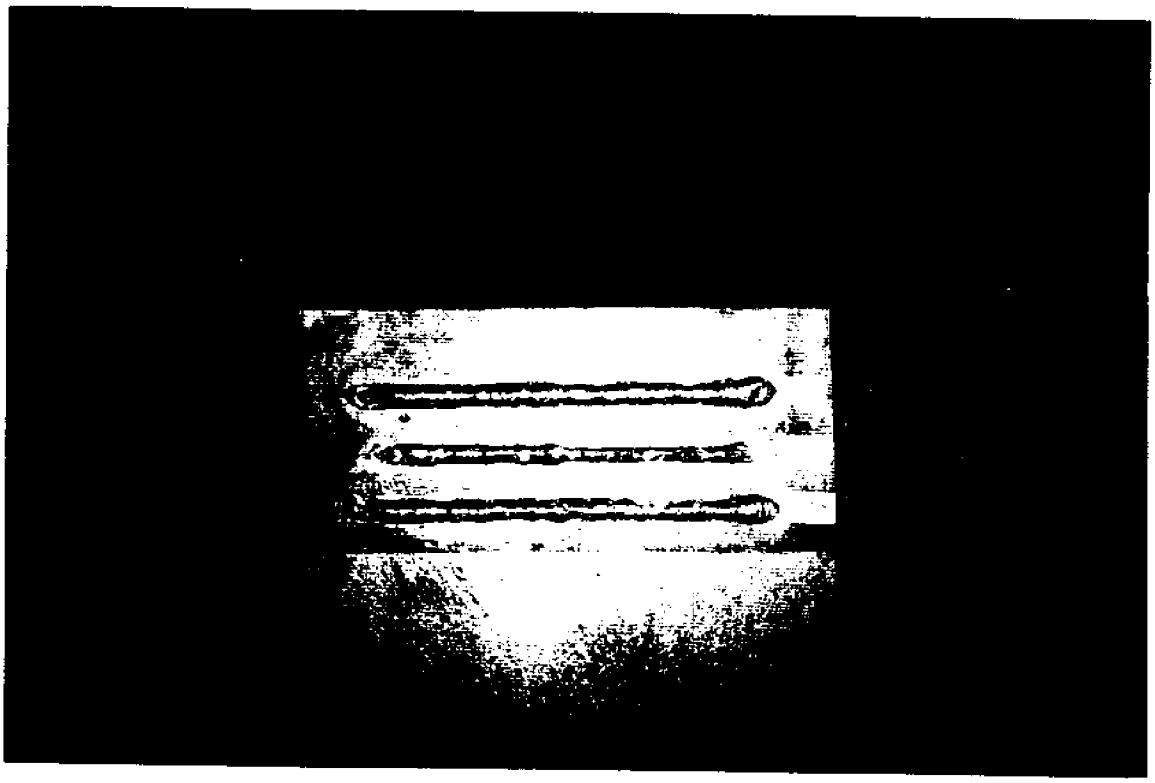

Figure 18 Bead Appearance of the Russian Welds

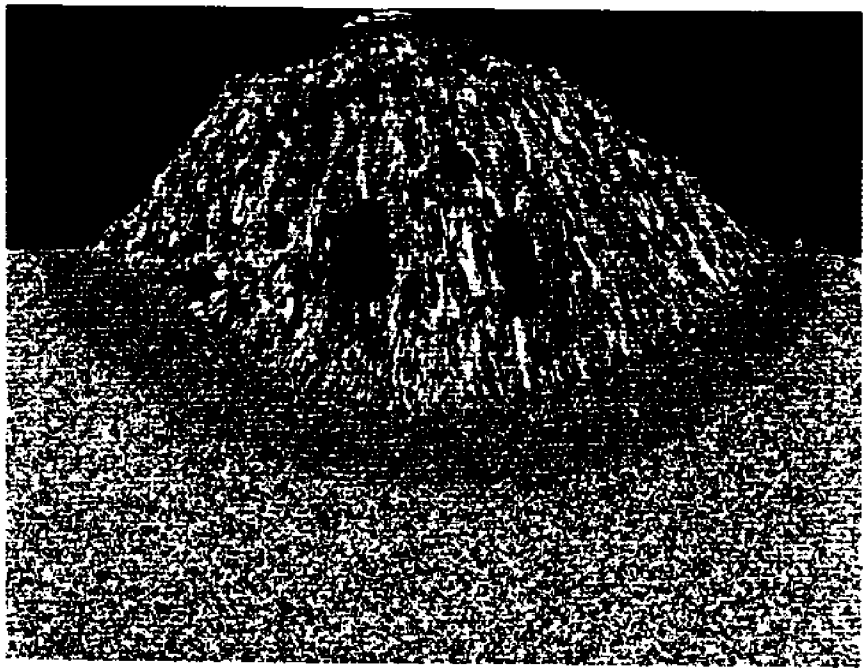

Figure 19 Cross Section of the Russian Weld(air weld) 10X

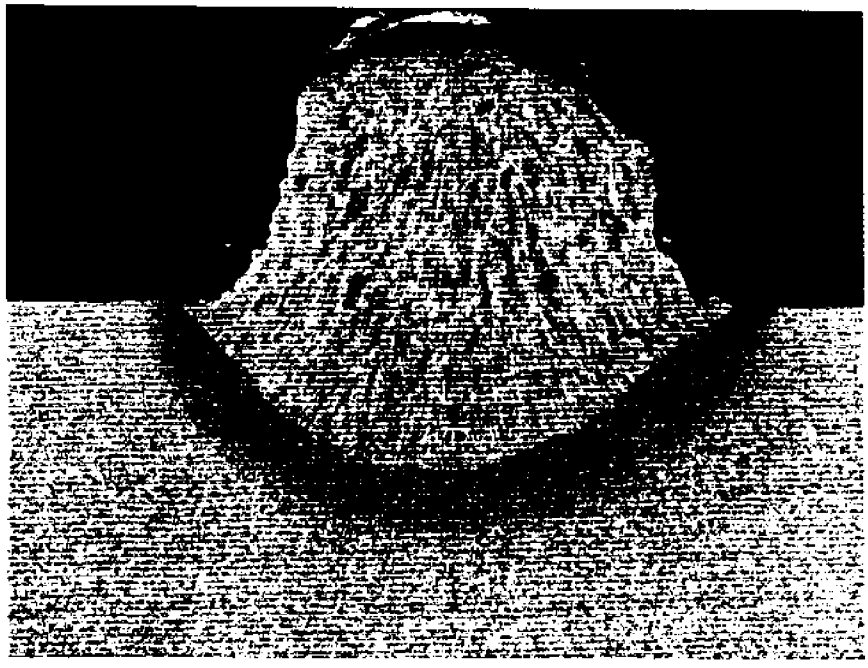

Figure 20 Cross Section of the Russian Weld(underwater weld without gas cup unit) 10X

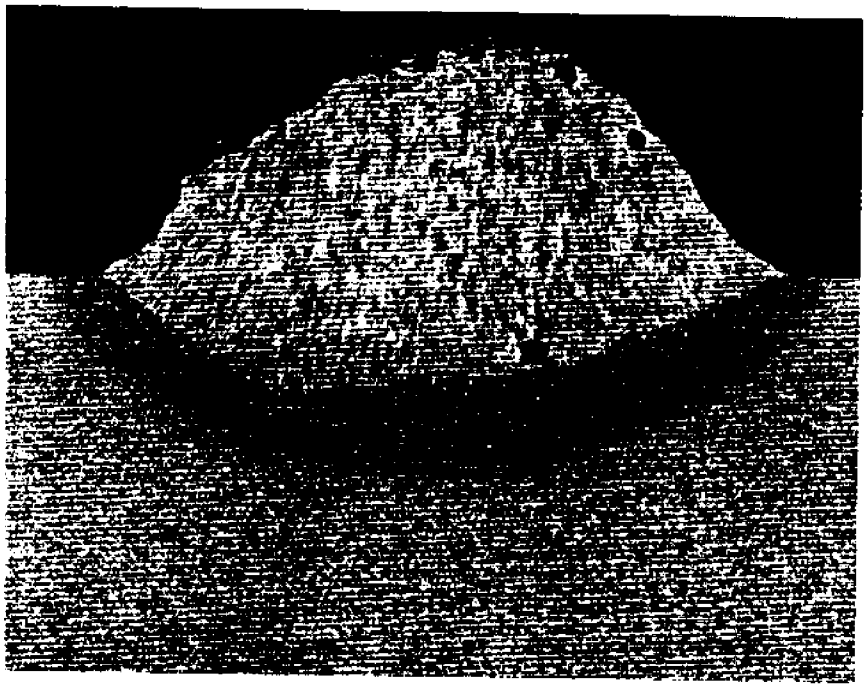

Figure 21 Cross Section of the Russian Weld(underwater weld with gas cup unit) 10X

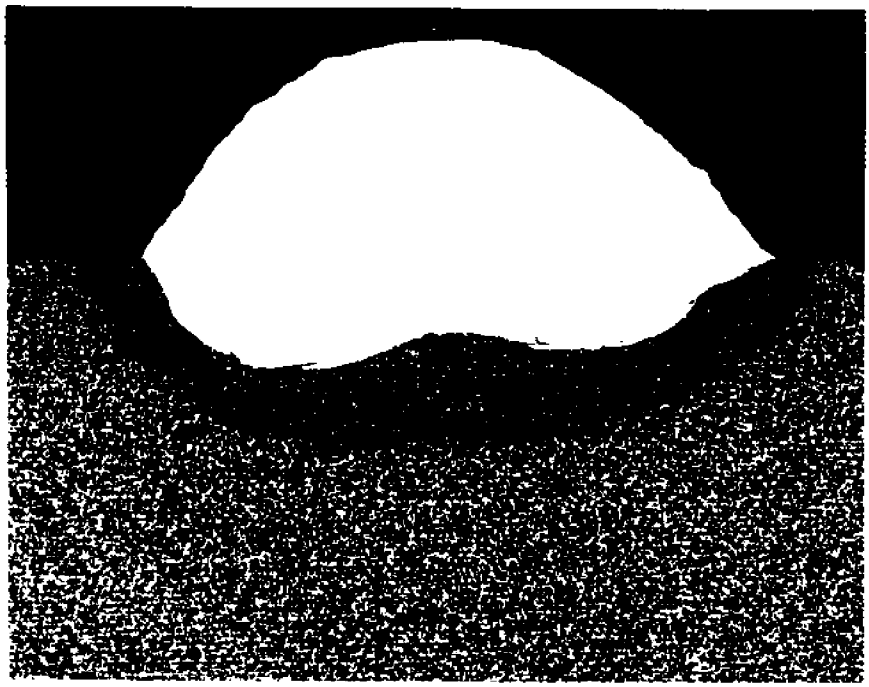

Figure 22 Cross Section of the SOS 308L Weld(air weld) 10X

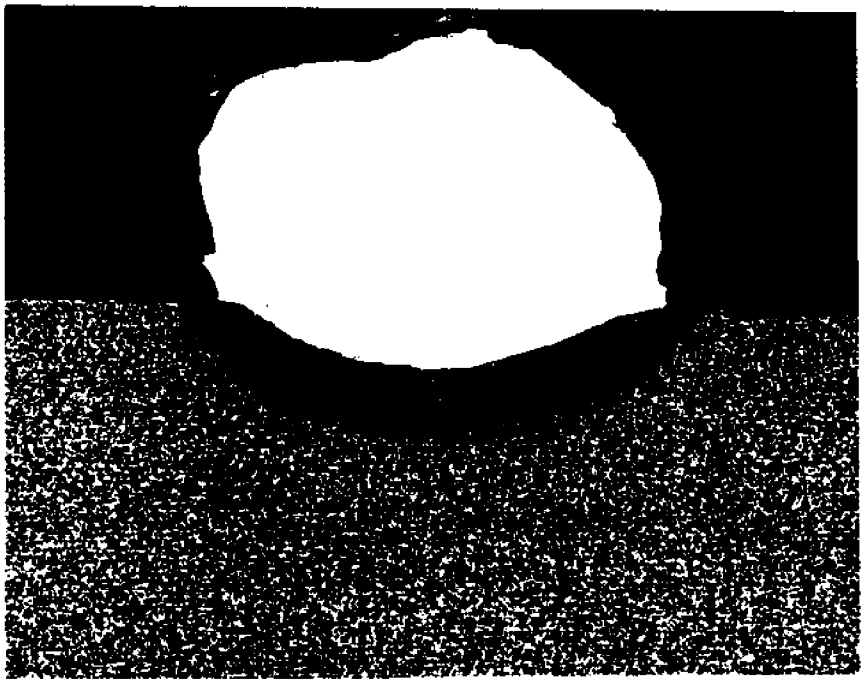

Figure 23 Cross Section of the SOS 308L Wire(underwater weld without gas cup unit) 10X

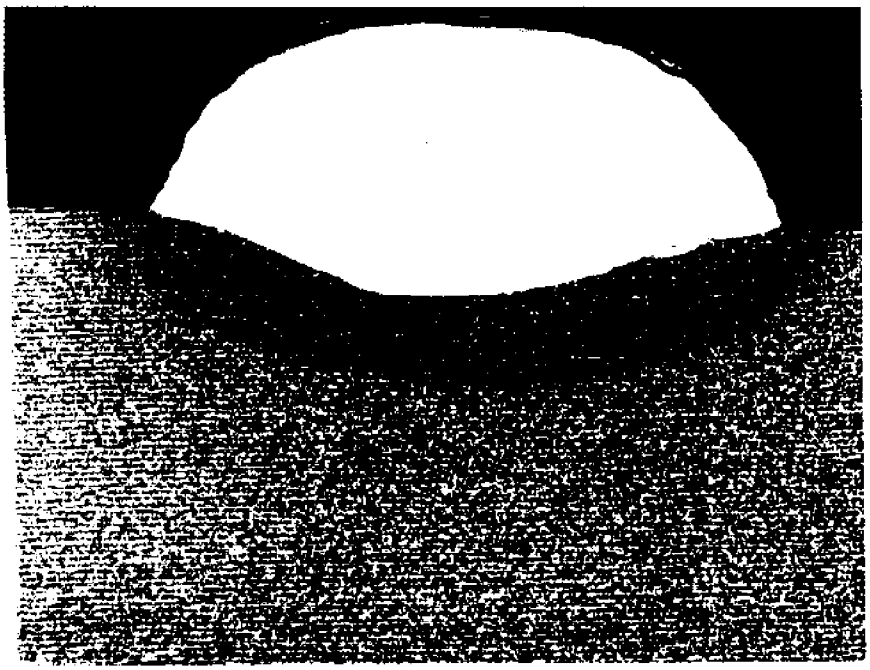

Figure 24 Cross Section of the SOS 308L Weld(underwater weld with gas cup unit) 10X

Figure 25 Weld Metal Microstructure of the Russian Wire(air weld) 200X

Figure 26 Weld Metal microstructure of the Russian Wire
(underwater weld without gas cup unit) 200X

Figure 27 Fusion Boundary Microstructures of the Russian Weld (underwater weld without gas cup unit) 200X

Figure 28 Weld Metal Microstructure of the Russian Wire (underwater weld with gas cup unit) 200X

Figure 29 Fusion Boundary Microstructures of the Russian Wire (underwater weld with gas cup unit) 200X

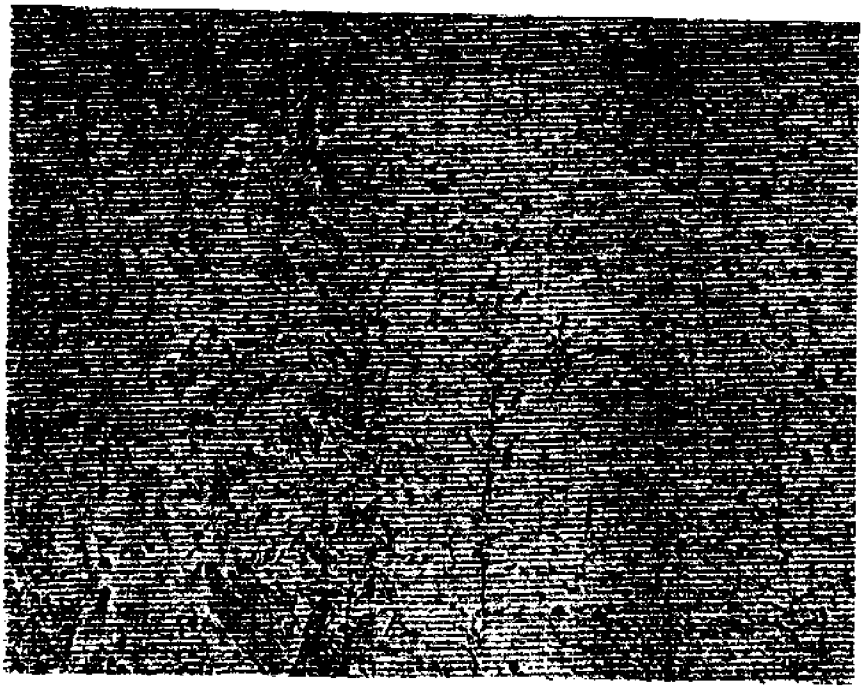

Figure 30 Weld Metal Microstructure of the SOS 308L Wire(air weld) 200X

Figure 31 Microstructures near Interface of the SOS 308L Weld(air weld) 400X

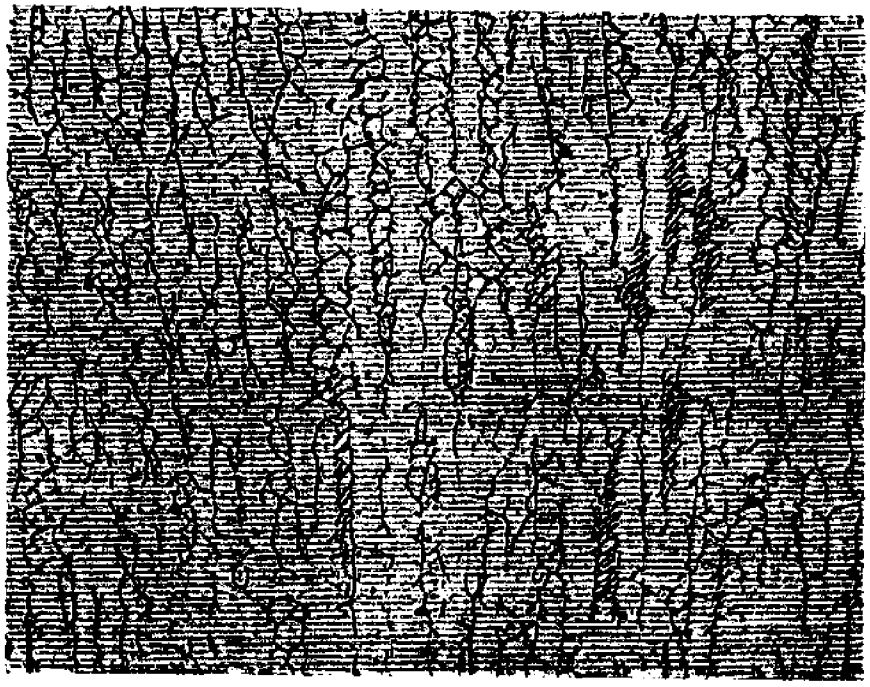

Figure 32 Weld Metal Microstructure of the SOS 308L Wire
(underwater weld without gas cup unit) 400X

Figure 33 Microstructure near Interface of the SOS 308L Weld
(underwater weld without gas cup unit) 400X

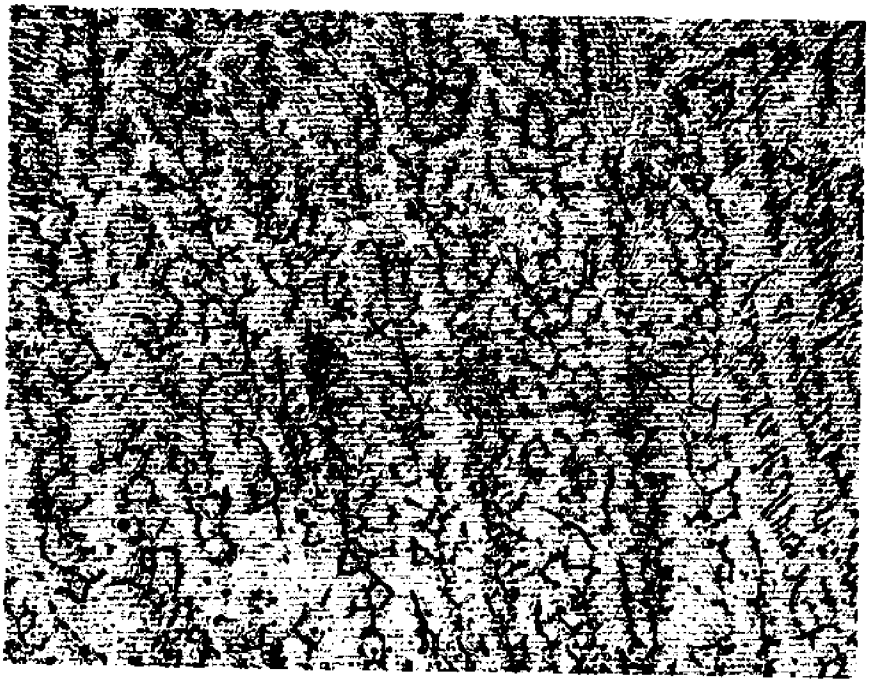

Figure 34 Weld Metal Microstructure of the SOS 308L Wire
(underwater weld with gas cup unit) 400X

Figure 35 Microstructures near Interface of the SOS 308L Weld (underwater weld with gas cup unit) 400X

a. Ferritic steel (Russian) weld, underwater.

b. Austenitic stainless steel (Stoody) weld, underwater

c. Austenitic stainless steel (Stoody) weld, air weld

Figure 36 All Weld Metal Tensile Test Samples of Different Welds

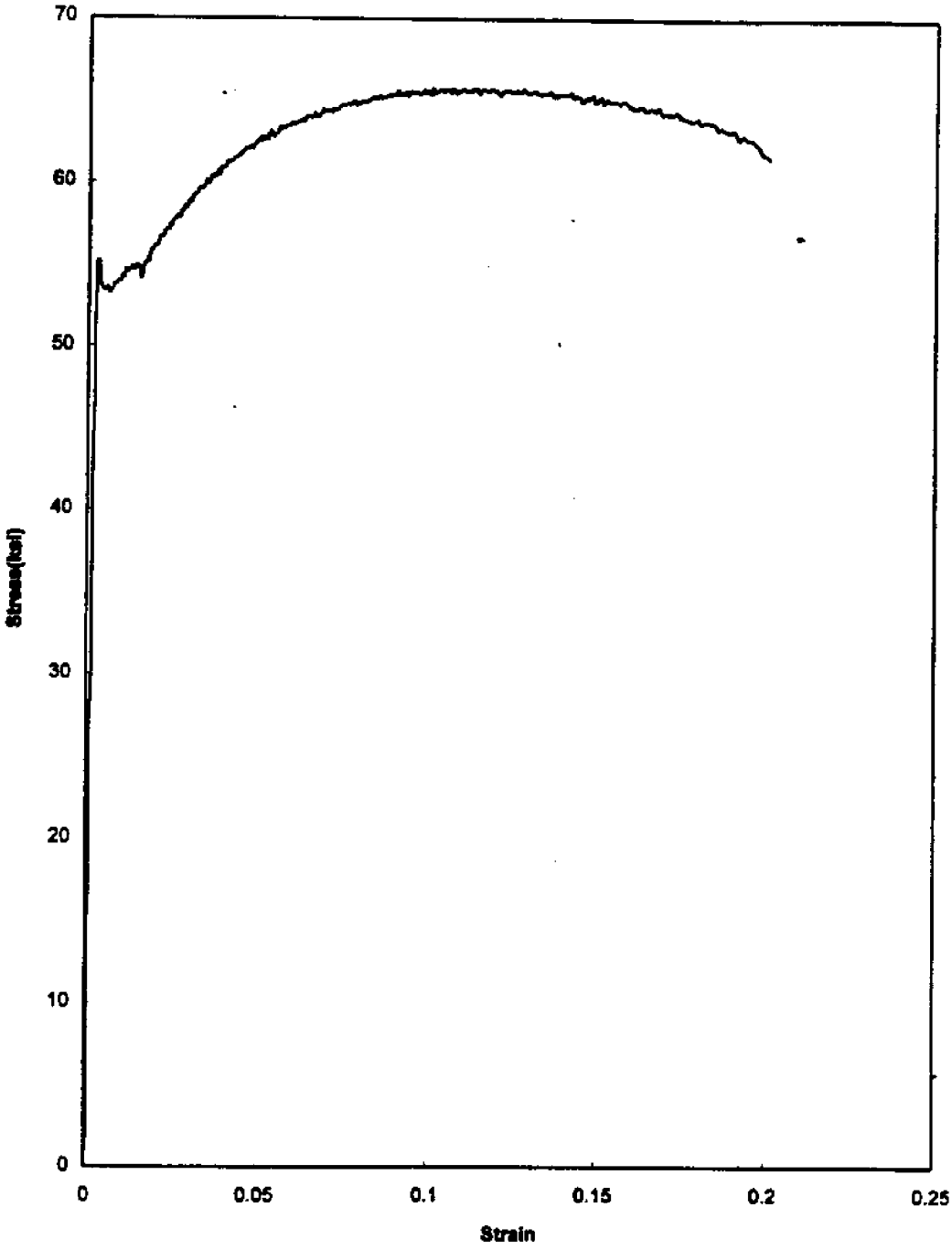

Figure 37 All Weld Metal Stress Strain Curve of the Russian FCAW Wire

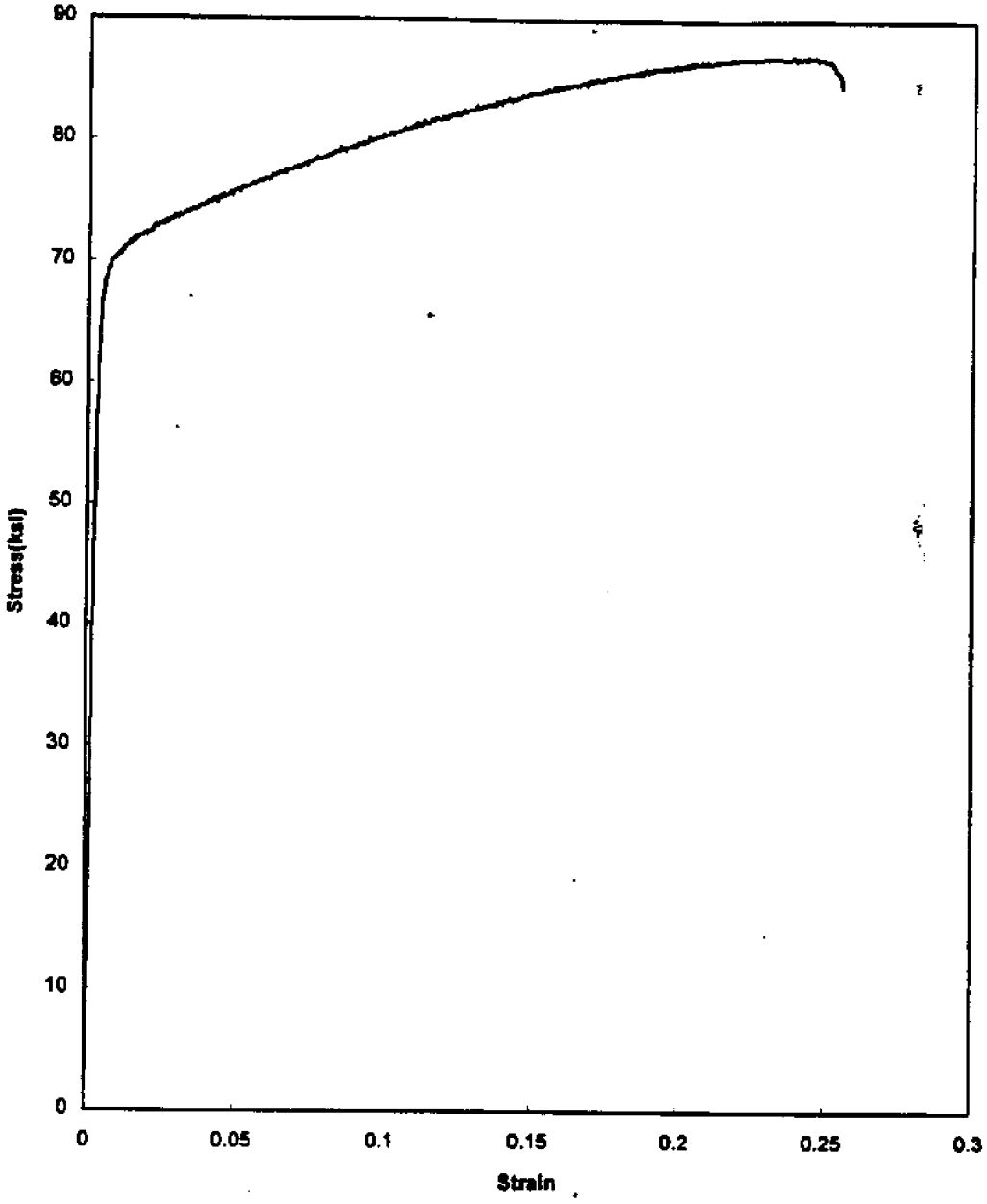

Figure 38 All Weld Metal Stress Strain Curve of the Stoody FCAW Wire (underwater weld)

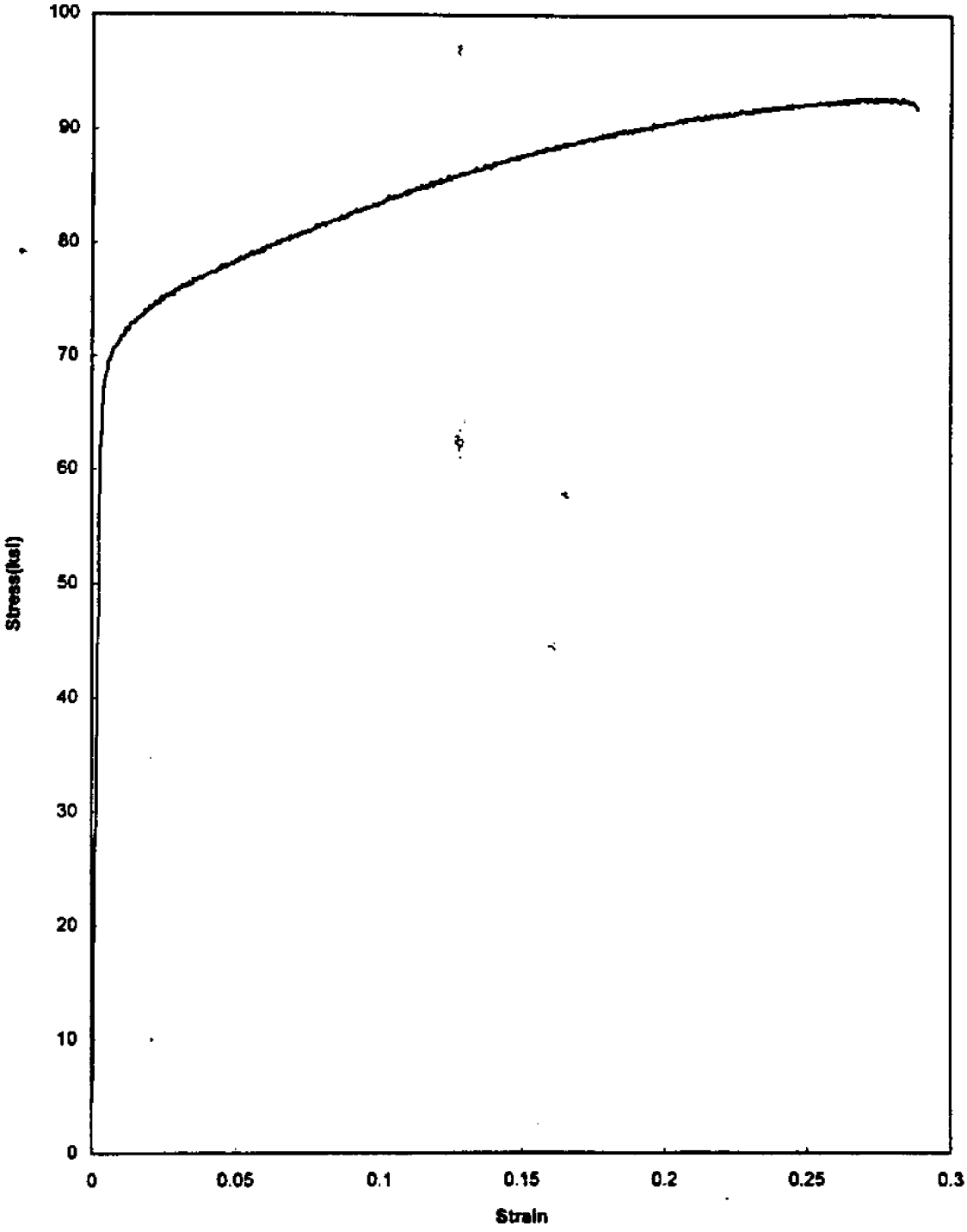

Figure 39 All Weld Metal Stress Strain Curve of the Stoody FCAW Wire (air weld)

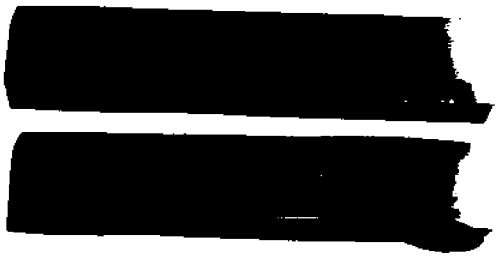

a. 2t, broken

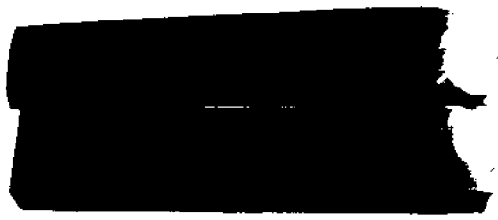

b. 4t, broken

c. 4t, bending angle: 30°

d. 4t, bending angle: 40°

Figure 40 Side Bend Test Samples of Ferritic Steel (Russian) Underwater Welds

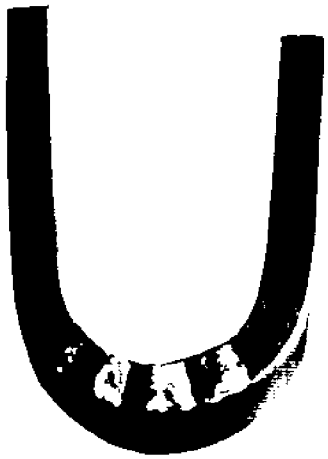

a. 4t, bending angle: 180°.

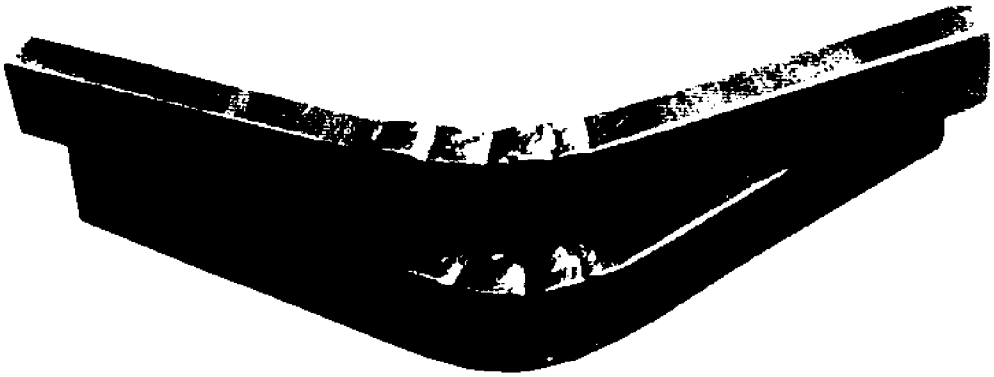

b. 4t, bending angle: 40°(upper sample) and 65°(lower sample)

c. 4t, bending angle: 40°

Figure 41 Side Bend Test Samples of Austenitic Stainless Steel (Stoody) Underwater Welds

a. Ferritic steel (Russian wire)underwater weld

b. Austenitic stainless steel (Stoody wire)underwater weld

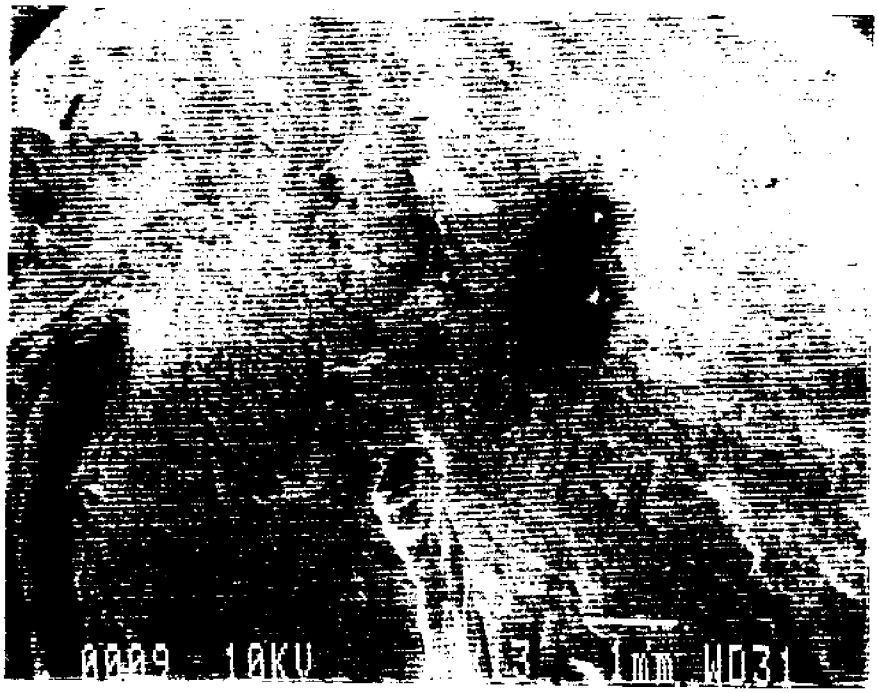

c. Austenitic stainless steel (Stoody wire) air weld

Figure 42 Fracture Surfaces of Different Welds(from AWT samples), 13X

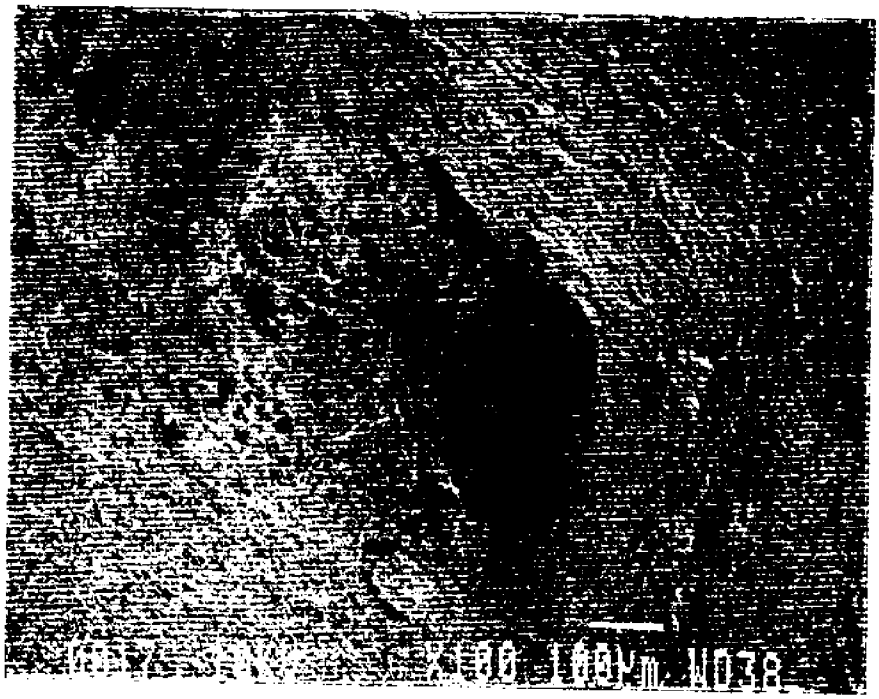

a. 100X

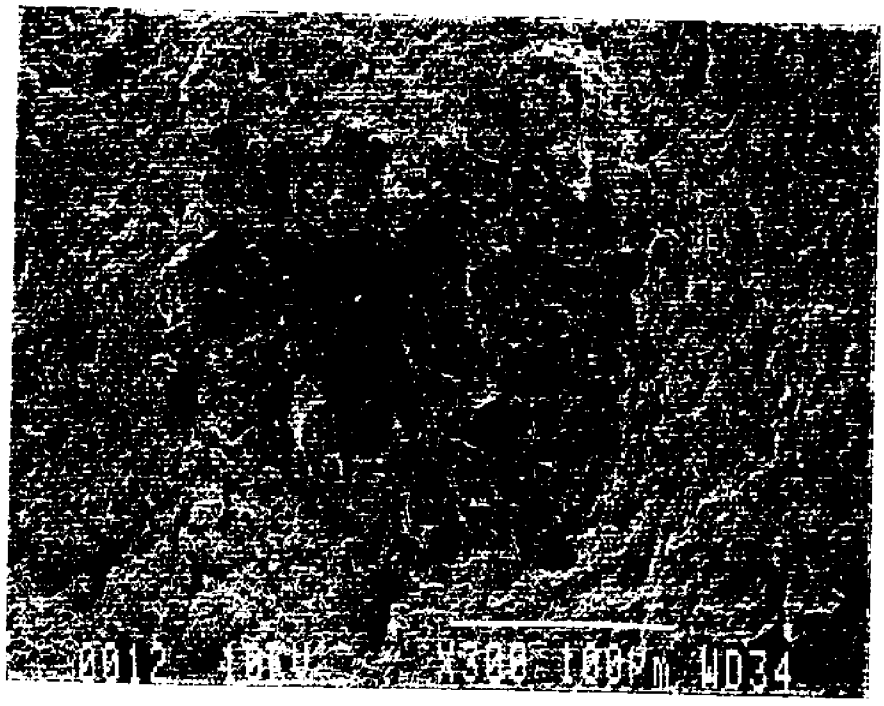

b. 300X

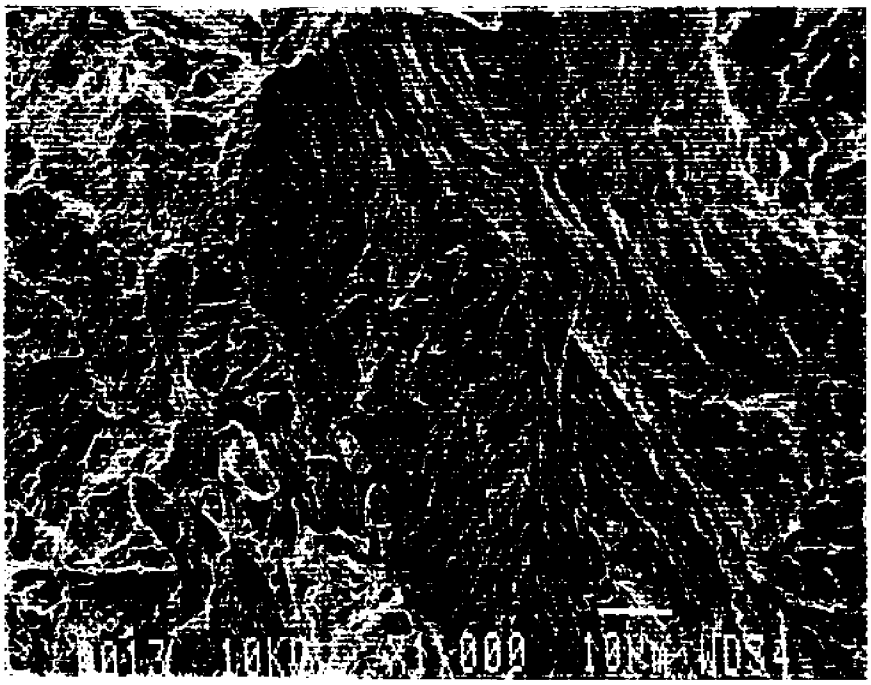

c. details inside the fisheye, 1000X

Figure 43 Fisheyes in Fracture Surfaces of Ferritic (Russian wire)Underwater Welds (from AWT sample)

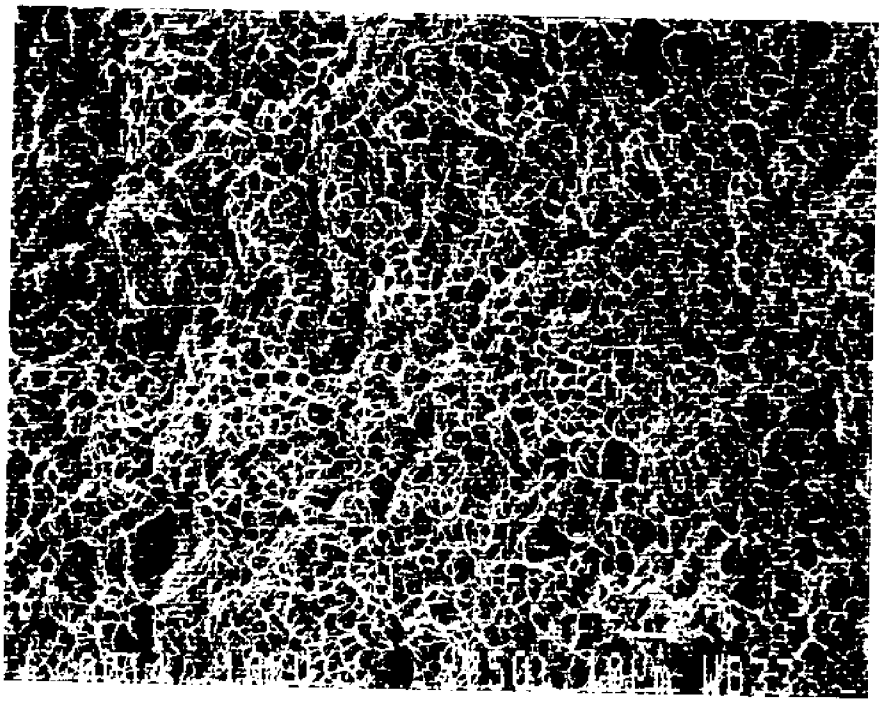

a. Ferritic steel (Russian wire)underwater weld

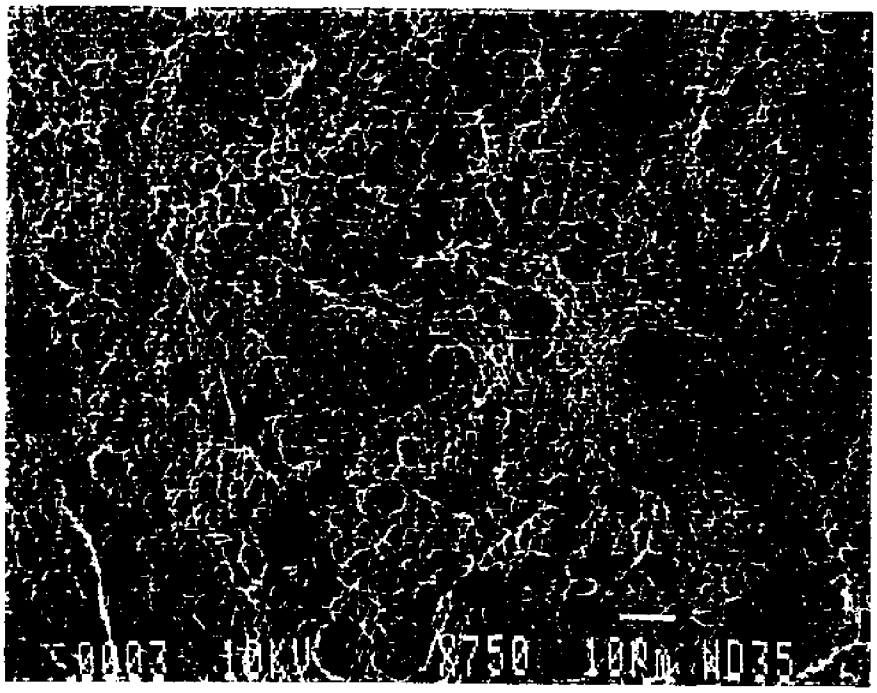

b. Austenitic stainless steel (Stoody wire)underwater weld

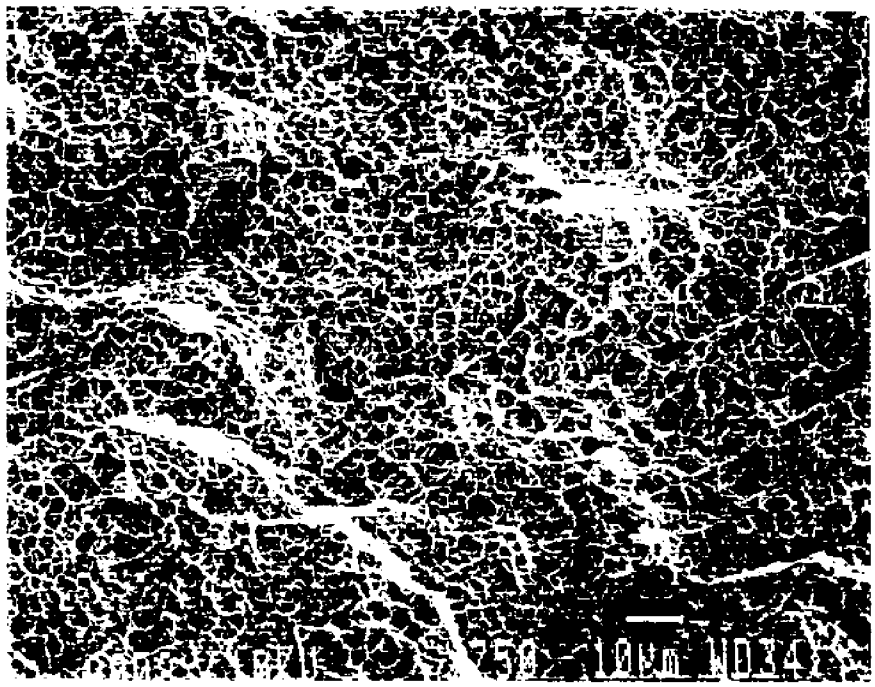

c. Austenitic stainless steel (Stoody wire) air weld

Figure 44 Ductile Fracture Morphology in Fracture Surfaces of Different Welds (from AWT samples), 750X

a. Ferritic steel (Russian wire)weld, 150X

b. Austenitic stainless steel (Stoody wire)weld, 130X

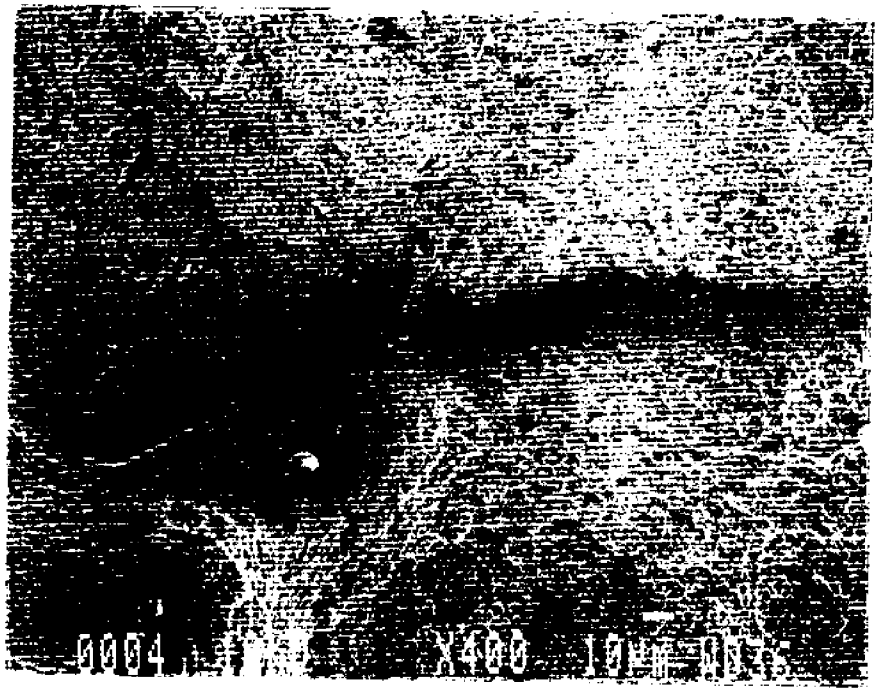

c. Austenitic stainless steel (Stoody wire)weld, 400X

Figure 45 Subcracks in Fracture Surfaces of Different Underwater Welds (from AWT samples), 750X

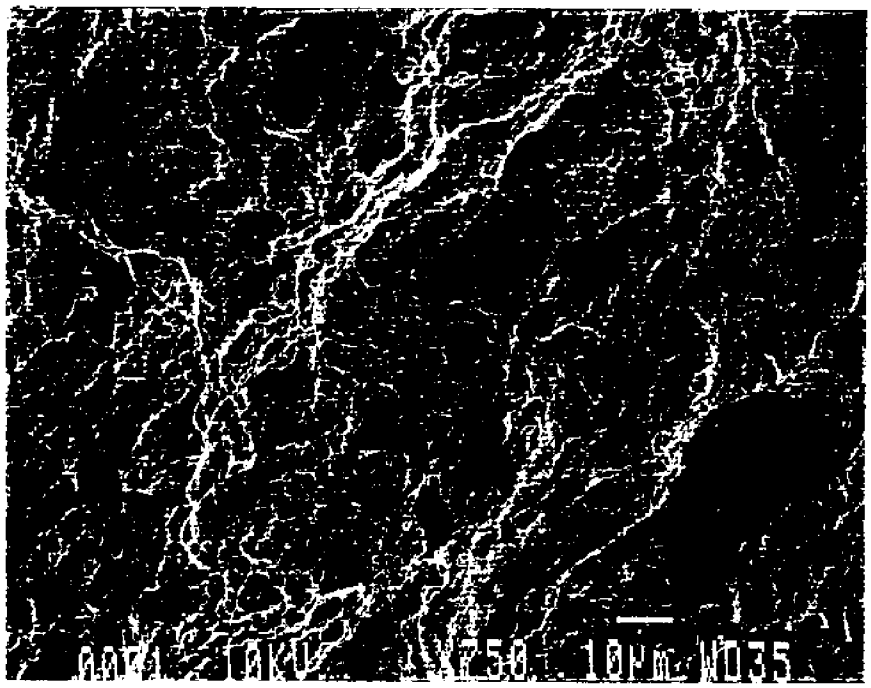

Figure 46 Ductile and Quasi-cleavage Morphologies in Fracture Surface of Austenitic Stainless Steel(Stoody wire) Underwater Weld(from AWT samples), 750X